

Lorentz and CPT violation and the hydrogen and antihydrogen molecular ions I – rovibrational states

Graham M. Shore

Department of Physics, Faculty of Science and Engineering, Swansea University, Singleton Park, Swansea, SA2 8PP, UK

E-mail: g.m.shore@swansea.ac.uk

ABSTRACT: The extremely narrow natural linewidths of rovibrational energy levels in the molecular hydrogen ion H_2^+ , and the prospect of synthesising its antimatter counterpart $\bar{\text{H}}_2^-$, make it a promising candidate for high-precision tests of fundamental symmetries such as Lorentz and CPT invariance. In this paper, we present a detailed analysis of the rovibrational spectrum of the (anti-)hydrogen molecular ion in a low-energy effective theory incorporating Lorentz and CPT violation. The focus is on the spin-independent couplings in this theory, and especially the CPT odd couplings for which the best current bounds come from measurements of the $1S-2S$ transition in atomic hydrogen and antihydrogen. We show that in addition to the improvement in these bounds from the increased precision of the transition frequencies, potentially reaching 1 part in 10^{17} , rovibrational transitions in the H_2^+ and $\bar{\text{H}}_2^-$ molecular ions have an enhanced sensitivity to Lorentz and CPT violation of $O(m_p/m_e)$ in the proton (hadron) sector compared to H and $\bar{\text{H}}$ atomic transitions.

1 Introduction

Local relativistic quantum field theories are the foundation of our current understanding of elementary particle physics. Together with microcausality, their basic principles of locality and Lorentz invariance imply the existence of antimatter and the necessity of CPT invariance as an exact symmetry of nature [1–4].

Given their essential rôle in our current theories, it is crucial that these fundamental principles – Lorentz invariance, CPT symmetry and locality – are tested experimentally to the highest possible precision [5]. To achieve such ultimate standards of precision, however, it is necessary to look beyond high-energy particle physics experiments to fundamental atomic physics, especially spin-precession measurements on elementary particles and atomic spectroscopy. For example, by comparing cyclotron frequencies, the BASE experiment at CERN has established the equality of the charge-to-mass ratios of the proton and antiproton to 16 parts in 10^{12} [6], while the ALPHA collaboration has measured the equality of the $1S$ - $2S$ transition in antihydrogen with that of hydrogen to 2 parts in 10^{12} [7], both key tests of CPT invariance.

The progress made in recent years by ALPHA in cooling, trapping and investigating antihydrogen has opened an era of high precision anti-atom spectroscopy, and future developments will push towards the benchmark precision of $O(10^{-15})$ achieved for the $1S$ - $2S$ transition in hydrogen. Already several transitions have been studied in detail, including $1S$ hyperfine [8] and $1S$ - $2P$ [9] transitions in addition to $1S$ - $2S$ [7, 10], and the results interpreted theoretically in terms of constraints on CPT violation.

In this paper, building on the work of [11], we extend the theoretical analysis of Lorentz and CPT symmetry breaking from (anti-)atoms to (anti-)molecules, in particular the molecular hydrogen ion H_2^+ and its antimatter counterpart, $\bar{\text{H}}_2^-$. The compelling feature of molecular ions for precision tests of fundamental symmetries is the existence of long-lived, extremely narrow linewidth, *rovibrational* states in which the two bound (anti-)protons make transitions between energy levels E_{vN} characterised by discrete vibrational and orbital angular momentum states, labelled here by v and N respectively.¹

These rovibrational transitions offer the possibility in principle of testing Lorentz and CPT invariance at up to $O(10^{-17})$ [14, 15]. In addition, as we show here, the nature of rovibrational states of the bound protons makes it possible to isolate the potential violation of Lorentz and CPT invariance in the proton (or more generically, hadron)

¹For a comprehensive recent review see [12]; earlier work is described in [13].

sector from the combined electron-proton effect observable in atomic spectroscopy. We show here that this feature alone gives an enhancement of $O(m_p/m_e) \sim 10^3$ in the precision of constraints on CPT violation from rovibrational transitions with molecular ions compared to those possible with atoms alone.

The theoretical framework we use to discuss Lorentz and CPT violation is a low-energy effective theory in which the QED Lagrangian is extended to include Lorentz tensor operators with fixed couplings. These couplings may be thought of as the vacuum expectation values of new tensor fields which, unlike the familiar case of the scalar Higgs field VEV, necessarily spontaneously break Lorentz, and in some cases also CPT, symmetry.

This framework is more generally known as the Standard Model Extension (SME) [16, 17] and for many years has been used extensively to systematise constraints on Lorentz and CPT symmetry breaking from a wide variety of experimental data [18]. In the form we use in this paper, the Lagrangian for a single Dirac fermion field $\psi(x)$ is extended to include a set of Lorentz tensor operators as follows:

$$\begin{aligned} \mathcal{L}_{\text{SME}} = & \frac{1}{2} \int d^4x \left[\bar{\psi} (i\gamma^\mu \partial_\mu - m) \psi - a_\mu \bar{\psi} \gamma^\mu \psi + ic_{\mu\nu} \bar{\psi} \gamma^\mu \partial^\nu \psi + a_{\mu\nu\lambda} \bar{\psi} \gamma^\mu \partial^\nu \partial^\lambda \psi \right. \\ & \left. - b_\mu \bar{\psi} \gamma^5 \gamma^\mu \psi + id_{\mu\nu} \bar{\psi} \gamma^5 \gamma^\mu \partial^\nu \psi - \frac{1}{2} H_{\mu\nu} \bar{\psi} \sigma^{\mu\nu} \psi + \frac{1}{2} ig_{\mu\nu\lambda} \bar{\psi} \sigma^{\mu\nu} \partial^\lambda \psi + \dots \right] \\ & + \text{h.c.} \end{aligned} \tag{1.1}$$

To understand the structure of the SME couplings, recall that the standard basis for the 16 possible 4×4 matrices acting on the Dirac spinor is $\Gamma = \mathbf{1}, \gamma^5, \gamma^\mu, \gamma^5 \gamma^\mu, \sigma^{\mu\nu}$, respectively scalar, pseudoscalar, vector, axial vector and tensor. The basic operators then take the form $\bar{\psi} \Gamma \psi$, and we can then add increasing numbers of derivatives, which increases the dimension of the operator.

Restricting to operators with dimension ≤ 4 leaves the theory renormalisable, just like the Standard Model itself. This restriction is known as the minimal SME. If on the other hand the SME is regarded as a low-energy effective theory, valid below some very high energy scale Λ , then we may include higher-dimensional operators. The corresponding couplings, such as $a_{\mu\nu\lambda}$, have negative mass dimensions. Here, we keep only the renormalisable couplings in the expansion (1.1) except for the inclusion of the coupling $a_{\mu\nu\lambda}$ of the higher dimensional operator $\bar{\psi} \gamma^\mu \partial^\nu \partial^\lambda \psi$, since this gives the leading spin-independent contribution to the difference of the H_2^+ and $\bar{\text{H}}_2^-$ spectra. As usual we assume that like the electron, the proton itself is effectively described by

this Lagrangian, with its own distinct couplings, despite it being a bound state of the fundamental quarks,

In this paper, our main focus is on the ‘spin-independent’ couplings $c_{\mu\nu}$ and $a_{\mu\nu\lambda}$ (so-called because in the non-relativistic limit they do not couple to the spin operator; see (3.1)), though we comment on spin and the hyperfine structure of H_2^+ and $\overline{\text{H}}_2^-$ in section 7. These couplings are not observable in spin precession experiments and are therefore much less stringently constrained than the remaining, spin-dependent, couplings b_μ , $d_{\mu\nu}$, $H_{\mu\nu}$ and $g_{\mu\nu\lambda}$. Indeed the best existing laboratory constraint on the CPT violating coupling $a_{\mu\nu\lambda}$ comes from the ALPHA antihydrogen $1S$ - $2S$ measurement.

The SME has important advantages in analysing potential violations of Lorentz and CPT symmetry. It provides a systematic parametrisation of possible symmetry breaking effects in terms of a standard set of couplings, which allows quantitative comparisons between experiments. It also makes it very clear that Lorentz and CPT violation may occur in many different ways and show up in some experimental measurements while remaining entirely hidden in others.

For example, it is entirely possible for CPT violation to be absent in the antihydrogen $1S$ - $2S$ transition, yet appear in transitions such as $1S$ - $2P$ involving states with non-zero orbital angular momentum, since these involve different SME couplings (see section 7). This is an important motivation to pursue an extensive programme of high-precision measurements of many different spectral transitions in H and $\overline{\text{H}}$, also including searching for sidereal and annual variations of the transition frequencies which would be a clear indication of Lorentz violation.

On the other hand, the symmetry breaking realised in the SME is comparatively mild and, as we have mentioned above, can be interpreted as spontaneous symmetry breaking in a theory which maintains all the essential features of local relativistic QFT, including Lorentz covariance. In particular, the usual equality of masses of particles and antiparticles (and of course their identical, but opposite, charges) is maintained in the SME, since the Lagrangian (1.1) is built on the original local causal fields of QED. We should therefore keep an open mind about more radical alternatives, including non-local theories, even though they generally lead more immediately to fundamental problems with unitarity and causality (see, for example, [5]).

The analysis of the molecular H_2^+ ion described here is based on the traditional Bohr-Oppenheimer approximation, in which the 3-body problem is separated into two Schrödinger equations. The first describes the electron wavefunction at fixed nucleon

separation R . The corresponding energy eigenvalues are then interpreted as an inter-nucleon potential $V_M(R)$ (Fig. 1) in a second Schrödinger equation describing the rovibrational motion of the nucleons. The SME is introduced perturbatively as a non-relativistic Hamiltonian (see (3.1)) derived from the Lagrangian (1.1).

The application of the SME to the hydrogen molecule and molecular ion has been previously studied in [11] (see also [19]). In this paper, we develop and extend this work in a number of important respects. First, we develop a systematic perturbation theory to determine the rovibrational energy levels and their SME corrections in terms of the potential $V_M(R)$ including anharmonic contributions. We see how these are essential to give an accurate characterisation of the rovibrational energy spectrum from which to evaluate the contribution of the SME couplings.

Most importantly, we include the Lorentz and CPT violating couplings for the protons, as well as the electron, which were not considered in [11, 19]. These have two rôles. Along with the electron SME couplings, they modify the inter-nucleon potential and consequently the rovibrational energies. The dependence on the electron and proton SME couplings from this mechanism is identical to that encountered already in the single atom energy levels. However, the proton couplings also enter directly in the nucleon Schrödinger equation. We show here that the different mass dependence of the coefficients of the SME couplings in this case results in the $O(m_p/m_e)$ enhancement in sensitivity to CPT violation in the proton sector highlighted above.

We present our results in terms of the following expansion of the rovibrational energy levels:

$$\begin{aligned}
 E_{vNM_N} = & V_{\text{SME}}^e + (1 + \delta_{\text{SME}}) (v + \tfrac{1}{2}) \omega_0 - (x_0 + x_{\text{SME}}) (v + \tfrac{1}{2})^2 \omega_0 \\
 & + (B_0 + B_{\text{SME}}) N(N + 1) \omega_0 - (D_0 + D_{\text{SME}}) (N(N + 1))^2 \omega_0 \\
 & - (\alpha_0 + \alpha_{\text{SME}}) (v + \tfrac{1}{2}) N(N + 1) \omega_0 + \dots
 \end{aligned} \tag{1.2}$$

We show that the coefficients here satisfy a hierarchy in terms of the small dimensionless parameter $\lambda = 2/(m_p \omega_0 R_0^2) = 0.027$ (where ω_0 is the fundamental vibration frequency and R_0 is the mean bond length in the absence of centrifugal and SME corrections), with $\delta_0, x_0, B_0, \alpha_0, D_0$ of order 1, $\lambda, \lambda, \lambda^2, \lambda^3$ respectively. Each of these coefficients is itself a perturbative expansion in λ^2 .

The SME coefficients $\delta_{\text{SME}}, B_{\text{SME}}, \dots$ are themselves the sum of electron and proton parts, reflecting the two ways described above in which the SME couplings influence the rovibrational spectrum. We determine explicitly how these coefficients depend on

certain combinations of the spin-independent SME couplings $c_{\mu\nu}$ and $a_{\mu\nu\lambda}$ in the Lagrangian (1.1). In a standard spherical tensor notation [17], these are denoted $c_{200}^{\text{NR}w}$, $a_{200}^{\text{NR}w}$, $c_{220}^{\text{NR}w}$, and $a_{220}^{\text{NR}w}$, where $w = e, p$. Of these, the (200) couplings are constrained by the two-photon $1S$ - $2S$ transitions in atomic H and $\bar{\text{H}}$, while the (220) only appear in the single-photon $1S$ - $2P$ transitions for which the natural linewidth is much broader and the constraint on the SME couplings correspondingly weaker. Both may be equally extracted from rovibrational transition data on the molecular ions H_2^+ and $\bar{\text{H}}_2^-$. The dependence on the (220) couplings introduces the M_N dependence in E_{vNM_N} and shows that even the spin-independent couplings contribute to the hyperfine-Zeeman levels for $N \neq 0$.

The paper is organised as follows. The Born-Oppenheimer approach is reviewed briefly in section 2 and extended to include the SME in section 3. Section 4 and Appendix A are devoted to solving the electron Schrödinger equation in the presence of the SME couplings, including numerical evaluations of the relevant expectation values. In section 5 and Appendix B we develop a systematic perturbation theory for calculating the SME contributions to the rovibrational energies for H_2^+ in terms of the inter-nucleon potential $V_M(R)$ and its derivatives in two complementary ways. Section 6 then describes the quantitative effect on the rovibrational spectrum.

Finally, in section 7 we take a first look at the rovibrational transitions arising from E_{vNM_N} in (1.2) in comparison with analogous results for electron transitions in single H and $\bar{\text{H}}$ atoms, and discuss the constraints on the SME couplings that could be obtained from measurements of rovibrational frequencies with H_2^+ and $\bar{\text{H}}_2^-$, including the search for sidereal and annual variations. We also comment briefly on the hyperfine-Zeeman spectrum, where both the spin-independent and spin-dependent SME couplings contribute to the energy levels. This is described in detail in a sequel to this paper [20], which we refer to as Paper 2.

2 Born-Oppenheimer analysis of the hydrogen molecular ion

We begin by reviewing the standard analysis of the spectrum of the hydrogen molecular ion H_2^+ in the Born-Oppenheimer approximation, before introducing Lorentz and CPT violation in section 3.

The starting point is the 3-body Schrödinger equation for the bound state. We denote the positions of the nucleons as \mathbf{r}_1 , \mathbf{r}_2 and the electron as \mathbf{r}_e , with corresponding momenta \mathbf{p}_1 , \mathbf{p}_2 and \mathbf{p}_e . For generality, we temporarily allow the masses m_1 and m_2 to be different in this section. The Hamiltonian is

$$H_{mol} = \sum_{w=1,2,e} \frac{p_w^2}{2m_w} + V_{mol}(R, r_{1e}, r_{2e}) , \quad (2.1)$$

with the electromagnetic potential,

$$V_{mol}(R, r_{1e}, r_{2e}) = \alpha \left(\frac{1}{R} - \frac{1}{r_{1e}} - \frac{1}{r_{2e}} \right) , \quad (2.2)$$

where $R = |\mathbf{r}_1 - \mathbf{r}_2|$, $r_{1e} = |\mathbf{r}_1 - \mathbf{r}_e|$, $r_{2e} = |\mathbf{r}_2 - \mathbf{r}_e|$ and α is the fine structure constant.

Next, we introduce CM variables for the coordinates and momenta. Iterating the standard construction for a 2-body system, we define

$$\begin{aligned} \mathbf{R} &= \mathbf{r}_1 - \mathbf{r}_2 , & \mathbf{r} &= \mathbf{r}_e - \frac{1}{M} (m_1 \mathbf{r}_1 + m_2 \mathbf{r}_2) \\ \mathbf{R}_{CM} &= \frac{1}{\hat{M}} (m_1 \mathbf{r}_1 + m_2 \mathbf{r}_2 + m_3 \mathbf{r}_3) , \end{aligned} \quad (2.3)$$

with $M = m_1 + m_2$ and $\hat{M} = m_1 + m_2 + m_e$, so that \mathbf{R} is the inter-nucleon separation, \mathbf{r} is the electron position relative to the nucleon CM, and \mathbf{R}_{CM} is the position of the CM of the whole molecule. The corresponding momenta are

$$\begin{aligned} \mathbf{P} &= \mu \dot{\mathbf{R}} = \frac{1}{M} (m_2 \mathbf{p}_1 - m_1 \mathbf{p}_2) , & \mathbf{p} &= \hat{\mu} \dot{\mathbf{r}} = \frac{1}{\hat{M}} (M \mathbf{p}_e - m_e (\mathbf{p}_1 + \mathbf{p}_2)) \\ \mathbf{P}_{CM} &= \hat{M} \dot{\mathbf{R}}_{CM} = \mathbf{p}_1 + \mathbf{p}_2 + \mathbf{p}_e , \end{aligned} \quad (2.4)$$

where we introduce the reduced masses $\mu = m_1 m_2 / M$ and $\hat{\mu} = m_e M / \hat{M}$. The relative motion of the nucleons is then treated as that of a single particle at position \mathbf{R} with momentum \mathbf{P} and reduced mass μ .

With these definitions,² the kinetic term in the Hamiltonian (2.1) becomes simply

$$\sum_{w=1,2,e} \frac{p_w^2}{2m_w} = \frac{1}{2\mu} P^2 + \frac{1}{2\hat{\mu}} p^2 + \frac{1}{2\hat{M}} P_{CM}^2 . \quad (2.5)$$

The Schrödinger equation for the molecule wavefunction $\Psi(\mathbf{R}, \mathbf{r}, \mathbf{R}_{CM})$ is therefore

$$\left(-\frac{1}{2\mu} \nabla_{\mathbf{R}^2} - \frac{1}{2\hat{\mu}} \nabla_{\mathbf{r}^2} - \frac{1}{2\hat{M}} \nabla_{\mathbf{R}_{CM}}^2 + V_{mol}(R, r_{1e}, r_{2e}) \right) \Psi(\mathbf{R}, \mathbf{r}, \mathbf{R}_{CM}) = E \Psi(\mathbf{R}, \mathbf{r}, \mathbf{R}_{CM}) . \quad (2.6)$$

Of course since we are not interested in the bulk motion of the molecule, from now on we set the CM momentum \mathbf{P}_{CM} to zero, and equivalently neglect the $\nabla_{\mathbf{R}_{CM}}^2$ term in (2.6).

The Born-Oppenheimer approximation³ now consists of separating the Schrödinger equation into two parts. Writing the molecular wave function $\Psi(\mathbf{R}, \mathbf{r}) = \Phi(\mathbf{R}) \psi(\mathbf{r}; R)$, we first solve the Schrödinger equation for the electron wavefunction $\psi(\mathbf{r}; R)$ for fixed nucleon separation R . The energy eigenvalues $E_e(R) \equiv V_M(R)$ then appear as a potential in the effective Schrödinger equation for the nucleons, which determines the rovibrational energy levels of the molecular ion. We therefore write the “electron Schrödinger equation”,

$$\left(-\frac{1}{2\hat{\mu}} \nabla_{\mathbf{r}}^2 + V_{mol}(R, r_{1e}, r_{2e}) \right) \psi(\mathbf{r}; R) = E_e(R) \psi(\mathbf{r}; R) . \quad (2.7)$$

We also restrict to the electron ground state $1s\sigma_g$. Substituting back into (2.6), the “nucleon Schrödinger equation” is then

$$\left(-\frac{1}{2\mu} \nabla_{\mathbf{R}}^2 + V_M(R) \right) \Phi(\mathbf{R}) = E \Phi(\mathbf{R}) . \quad (2.8)$$

Finally, exploiting the spherical symmetry of the molecular axis in the fixed frame of the experiment (denoted EXP, see section 3) to write $\Phi(\mathbf{R}) = \frac{1}{R} \phi(R) Y_{NM_N}(\theta, \phi)$ in terms of spherical harmonics, we find

$$\left(-\frac{1}{2\mu} \frac{d^2}{dR^2} + \frac{1}{2\mu R^2} N(N+1) + V_M(R) \right) \phi(R) = E_{vN} \phi(R) \quad (2.9)$$

²Notice that with these definitions, in contrast to defining the electron momentum relative to the geometric centre of the molecule, there are *no* mixed terms in the momenta of the form $\mathbf{P} \cdot \mathbf{p}$ in (2.5) and the Schrödinger equation (2.6) even for a heteronuclear molecule with $m_1 \neq m_2$.

³A detailed justification of the Born-Oppenheimer method may be found in most standard textbooks; see, for example, [21].

Here, we follow the widely-used convention of denoting the discrete vibrational energy states by the integer v and the nucleon angular momentum states by N, M_N , with M_N the 3-component with respect to the EXP frame.

An approximate solution to the electron Schrödinger equation, based on an R -dependent *ansatz* for the wavefunction $\psi(\mathbf{r}; R)$, is discussed in detail in Appendix A. The method is essentially standard, but we require some special features and numerical results which ultimately feed into the coefficients of the Lorentz and CPT violating couplings constrained by the rovibrational spectrum of the (anti-)molecular ion. Inserting the resulting R -dependent energy eigenvalues into the nucleon Schrödinger equation then gives an inter-nucleon potential of the typical Morse potential form illustrated in Fig. 1 in section 4.

For H_2^+ , this has a minimum at $R_0 \simeq 2a_0$ (where a_0 is the Bohr radius) about which the nucleons undergo approximately simple harmonic motion with angular frequency ω_0 and integer vibrational quantum number v . For H_2^+ , $\omega_0 \simeq 0.02 R_H$, where R_H is the Rydberg energy, 13.6 eV. The spherical symmetry implies that the rovibrational energy levels depend only on the nucleon orbital angular momentum quantum number N , and *not* the component M_N . As we see in the next section, however, this is no longer true when the Lorentz and CPT violating interactions are introduced.

Solving the nucleon Schrödinger equation then allows the rovibrational energy levels E_{vN} to be written as an expansion in $(v + \frac{1}{2})$ and $N(N + 1)$, *viz.*⁴

$$\begin{aligned}
 E_{vN} = & (v + \frac{1}{2})\omega_0 - x_0(v + \frac{1}{2})^2\omega_0 \\
 & + B_0 N(N + 1)\omega_0 - \alpha_0 (v + \frac{1}{2})N(N + 1)\omega_0 - D_0 (N(N + 1))^2\omega_0 + \dots,
 \end{aligned}
 \tag{2.10}$$

where $\omega_0^2 = V_M''(R_0)/\mu$. It will be very useful in organising this expansion to introduce the small dimensionless parameter $\lambda = 1/(\mu\omega_0 R_0^2)$, which for H_2^+ is $\lambda \simeq 0.027$. From (2.9) it follows directly that at leading order, $B_0 = \lambda/2$. In fact, all the coefficients are themselves power series in λ , determined by higher derivatives of the potential $V_M(R)$, with their leading terms displaying a hierarchy in this small parameter. In section 5, we show explicitly that the leading terms for x_0 , α_0 and D_0 are of order λ, λ^2 and λ^3 respectively.

Explicit analytic expressions for these coefficients will be given later, and evaluated numerically to a precision sufficient to determine the prefactors of the contributions of

⁴The notation here is relatively standard (see *e.g.* [22]), but note that we have taken out a common energy factor ω_0 so the coefficients $B_0, x_0, \alpha_0, D_0, \dots$ here are all dimensionless.

the Lorentz and CPT violating couplings to the rovibrational energy levels. Of course, extensive calculations in high-order QED carried out over many years have determined them to extremely high precisions of a few parts in 10^{12} , enabling direct comparisons of experiment with *ab initio* theory (see *e.g.* [23]), but this sort of precision is not needed for our purpose here.

3 Born-Oppenheimer analysis with Lorentz and CPT violation

In this section, we extend the Born-Oppenheimer analysis of the H_2^+ molecular ion to include the effects of possible Lorentz and CPT violation.

We start from the non-relativistic Hamiltonian derived from the SME Lagrangian (1.1) for a single Dirac fermion:

$$H_{\text{SME}}^{\text{NR}} = (A + 2 B_k S^k) + (C_i + 2 D_{ik} S^k) \frac{p^i}{m} + (E_{ij} + 2 F_{ijk} S^k) \frac{p^i p^j}{m^2}, \quad (3.1)$$

where S^k is the spin operator. Since QED conserves parity, the leading perturbative contributions to expectation values from C_i and D_{ij} vanish, while A gives only a common addition to the energy levels and does not affect the spectrum. In terms of the fundamental SME couplings, the relevant coefficients for spectroscopy are [17, 24, 25]

$$\begin{aligned} B_k &= -b_k + m d_{k0} + \frac{1}{2} \epsilon_{kmn} (H_{mn} - m g_{mn0}), \\ E_{ij} &= -m (c_{ij} + \frac{1}{2} c_{00} \delta_{ij}) + m^2 (3 a_{0ij} + a_{000} \delta_{ij}), \\ F_{ijk} &= \frac{1}{2} (b_k \delta_{ij} - b_j \delta_{ik}) + m (d_{0j} + \frac{1}{2} d_{j0}) \delta_{ik} - \frac{1}{4} \delta_{ik} \epsilon_{jmn} H_{mn} \\ &\quad - m \epsilon_{ikm} (g_{m0j} + \frac{1}{2} g_{mj0}). \end{aligned} \quad (3.2)$$

To keep the presentation reasonably simple, and because the spin-dependent couplings are experimentally already far more constrained than the spin-independent couplings, we discuss mainly the spin-independent effects in this paper. These arise from the coupling combinations E_{ij}^p , E_{ij}^e for the protons and electron respectively. The analysis of the spin-dependent contributions is then conceptually largely straightforward and will be briefly introduced in section 7, where we discuss some aspects of the spectrum including hyperfine-Zeeman splittings.

With the inclusion of the Lorentz violating couplings, we need to be especially careful in specifying the reference frame in which the components are defined. Altogether, there are four frames of reference which are relevant to our discussion of the

molecular ion. In order to compare constraints on the SME couplings between different experiments it has become standard practice to quote bounds ultimately in terms of a standard Sun-centred frame (SUN), which is in turn related to a “standard laboratory frame” (LAB). The precise definitions of these standard frames and the coordinate transformations relating them may be found, for example, in [19].

Here, we are mainly concerned with two further frames. An “apparatus frame” (EXP), with basis vectors \mathbf{e}_i ($i = 1,2,3$), is chosen which is specific to the particular experiment and, importantly, in which the angular momentum components considered below are defined. Typically it will be chosen such that the \mathbf{e}_3 basis vector is aligned with a background magnetic field. We define the nucleon rotational quantum numbers N, M_N with respect to this EXP frame. Importantly, the SME couplings E_{ij} are, as indicated by the indices, also expressed here in the EXP frame.

Finally, in particular in the solution of the electron Schrödinger equation, we will also work in a frame (MOL) with basis vectors \mathbf{e}_a ($a = x, y, z$) with the z -axis aligned with the inter-nucleon, or molecular, axis.

To implement the Born-Oppenheimer analysis in this theory, we first rewrite the SME Hamiltonian in terms of the CM momenta introduced above. For H_2^+ , the reduced masses are $\mu = m_p/2$ and $\hat{\mu} = m_e(1 + m_e/2m_p)^{-1}$ and we find, keeping only the E_{ij} couplings,

$$\Delta H_{\text{SME}} = \frac{2}{m_p^2} E_{ij}^p P^i P^j + \left(\frac{1}{2m_p^2} E_{ij}^p + \frac{1}{m_e^2} E_{ij}^e \right) p^i p^j . \quad (3.3)$$

Notice that there is no mixed momentum term proportional to $P^i p^j$ in this SME Hamiltonian. This is a special feature of the homonuclear case, where $m_1 = m_2$, and is not true for heteronuclear molecular ions such as HD^+ .

Splitting the Schrödinger equation for the molecule in the Born-Oppenheimer approximation as above, and evaluating throughout in the MOL frame, we therefore find

$$\left(-\frac{1}{2\hat{\mu}} \nabla_{\mathbf{r}}^2 + V_{\text{mol}}(R, r_{1e}, r_{2e}) + \left(\frac{1}{2m_p^2} E_{ab}^p + \frac{1}{m_e^2} E_{ab}^e \right) p^a p^b \right) \psi(\mathbf{r}; R) = E_e(\mathbf{R}) \psi(\mathbf{r}; R) , \quad (3.4)$$

where we understand $\mathbf{p} \rightarrow -i\nabla_{\mathbf{r}}$. We write $E_e(\mathbf{R}) \equiv V_M(R) + V_{\text{SME}}^e(\mathbf{R})$ here to remember that $V_{\text{SME}}^e(\mathbf{R})$ depends on the orientation (θ, ϕ) of the molecular axis in the EXP frame, but through the SME couplings alone. The relation of these couplings in the MOL and EXP frames is calculated in the next section.

The nucleon Schrödinger equation, which is expressed in the EXP frame, is then

$$\left(-\frac{1}{2\mu} \nabla_{\mathbf{R}}^2 + V_M(R) + V_{\text{SME}}^e(\mathbf{R}) + \frac{2}{m_p^2} E_{ij}^p P^i P^j \right) \Phi(\mathbf{R}) = E_{vNM_N} \Phi(\mathbf{R}) . \quad (3.5)$$

We see here that with the Lorentz and CPT breaking term $V_{\text{SME}}^e(\mathbf{R})$, the usual spherical symmetry of the unperturbed nucleon Schrödinger equation is broken. In turn, the degeneracy of the rovibrational energy levels at fixed N is broken and they acquire a dependence also on the quantum number M_N .

Notice also how, perhaps unexpectedly, the proton SME couplings appear already in the Schrödinger equation for the electron and so modify the effective potential for the nucleon motion as well as their direct appearance in (3.5). To simplify notation, from now on we use the abbreviated notation $\tilde{E}_{ij}^e = E_{ij}^e + \frac{1}{2}(m_e^2/m_p^2) E_{ij}^p$. Note that despite the small pre-factor, we should not immediately drop the second term as we have no *a priori* knowledge of the relative sizes of the SME couplings for different particles (see also section 7).

Next, expressing $\Phi(\mathbf{R})$ in terms of spherical harmonics as before, we may write the analogue of (2.9) as follows:

$$\left(-\frac{1}{2\mu} \frac{d^2}{dR^2} + \frac{1}{2\mu R^2} N(N+1) + V_M(R) + V_{\text{SME}}^e(R) \right) \phi(R) = \tilde{E}_{vNM_N} \phi(R) , \quad (3.6)$$

where

$$V_{\text{SME}}^e(R) = \langle NM_N | V_{\text{SME}}^e(\mathbf{R}) | NM_N \rangle = \int d\Omega Y_{NM_N}^*(\theta, \phi) V_{\text{SME}}^e(\mathbf{R}) Y_{NM_N}(\theta, \phi) . \quad (3.7)$$

The contribution of the E_{ij}^p term in (3.5) to the total rovibrational energies E_{vNM_N} is calculated in first order perturbation theory by evaluating $\langle P^i P^j \rangle$ in the unperturbed nucleon state. Defining

$$\Delta E_{\text{SME}}^n = \frac{2}{m_p^2} E_{ij}^p \langle v NM_N | P^i P^j | v NM_N \rangle , \quad (3.8)$$

we finally have

$$E_{vNM_N} = \tilde{E}_{vNM_N} + \Delta E_{\text{SME}}^n \quad (3.9)$$

In the following sections, we solve these equations and evaluate the SME corrections to the rovibrational energy levels.

4 Electron Schrödinger equation and inter-nucleon potential

We are now in a position to determine the inter-nucleon potential $V_M(R)$ by solving the electron Schrödinger equation (2.7). We then include the Lorentz and CPT breaking couplings and evaluate the potential $V_{\text{SME}}^e(R)$ in (3.6) and its consequent effect on the rovibrational energy levels.

The detailed calculations of the energy eigenvalues and momentum expectation values in the absence of Lorentz and CPT breaking are described in Appendix A, so here we just summarise the essential features. We start from the following *ansatz* for the electron wave function, as always in the $1s\sigma_g$ ground state,

$$\psi(\mathbf{r}; R) = \frac{1}{\sqrt{2(1 + I_0(R))}} (\psi_H(r_{1e}; R) + \psi_H(r_{2e}; R)) , \quad (4.1)$$

where

$$\psi_H(r; R) = \sqrt{\frac{\gamma(R)^3}{\pi \hat{a}_0^3}} e^{-\gamma(R)r/\hat{a}_0} . \quad (4.2)$$

and the overlap function $I_0(R)$ ensures the wavefunction is correctly normalised. The $\psi_H(r; R)$ are hydrogen $1s$ wavefunctions with reduced Bohr radius \hat{a}_0 , modified by an interpolating function $\gamma(R)$ which adjusts the effective Bohr radius according to the inter-nucleon separation R [11]. This function is determined numerically by minimising the energy eigenvalue $E_e(R)$ for each value of R . It is also constrained physically to take the values $\gamma(0) = 2$ and $\gamma(R) \rightarrow 1$ for large R . This ensures the wavefunction reduces to that of a hydrogen-like atom with $Z = 2$ as the nucleon separation goes to zero, while for large separations the molecule effectively separates into an isolated proton and a single hydrogen atom in the $1s$ state with the usual Bohr radius.

With $\gamma(R)$ set to 1, the energy eigenvalues may be calculated analytically in terms of elementary integrals, and we find a simple expression for $E_{e1}(R) = K_1(R) + U_1(R)$ in terms of the corresponding kinetic and potential energies, with

$$K_1(R) = \frac{1}{(1 + I_0)} \left(1 + (1 + R - \frac{1}{3}R^2)e^{-R} \right) , \quad (4.3)$$

and

$$U_1(R) = \frac{2}{R} - \frac{2}{(1 + I_0)} \left(1 + \frac{1}{R} + 2(1 + R)e^{-R} - \left(1 + \frac{1}{R}\right)e^{-2R} \right) , \quad (4.4)$$

where $I_0(R) = (1 + R + \frac{1}{3}R^2) \exp(-R)$.⁵ Reinstating $\gamma(R)$, the energy $E_e(R)$ may be deduced from these results by inspection, following through the appropriate rescalings.

⁵Here we are using atomic units (see Appendix A) where R is rescaled by the reduced Bohr radius \hat{a}_0 and is dimensionless and energies are similarly scaled by the reduced Rydberg constant \hat{R}_H .

This gives

$$E_e(R) = \gamma(R)^2 K_1(\gamma(R)R) + \gamma(R) U_1(\gamma(R)R) . \quad (4.5)$$

Inserting the interpolating function $\gamma(R)$ found numerically in Appendix A, $E_e(R)$ is plotted in Fig. 1. As anticipated, it takes the characteristic Morse-like form, with a minimum at $R_0 = 2.003 \hat{a}_0$. For small R , it is dominated by the inter-nucleon repulsion $2/R$ while otherwise $E_e(0) \rightarrow -4\hat{R}_H$, as appropriate for an atom with $Z = 2$. For large R we recover $E_e(R) \rightarrow E_{1s} = -\hat{R}_H$, the ground state energy of a hydrogen atom.

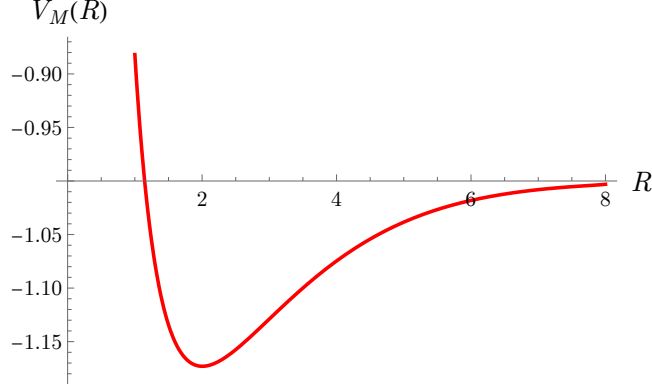


Figure 1. The nucleon potential $V_M(R) \equiv E_e(R)$ as the inter-nucleon distance, or bond length, R is varied. The minimum is at $R_0 = 2.003$ in units of the reduced Bohr radius \hat{a}_0 .

As explained above, in the Born-Oppenheimer approximation, the energy eigenvalue $E_e(R)$ is identified as the inter-nucleon potential $V_M(R)$. Its curvature at the minimum gives the fundamental vibrational frequency ω_0 of the molecule. We find

$$\omega_0 = \sqrt{\frac{1}{\mu} V_M''(R_0)} = 0.020 \hat{R}_H , \quad (4.6)$$

that is, $\omega_0 = 0.275$ eV.

The expectation values for the momentum, required to evaluate the potential $V_{\text{SME}}^e(R)$ are given by

$$\langle p^a p^b \rangle = - \int d^3 \mathbf{r} \psi(\mathbf{r}; R) \nabla^a \nabla^b \psi(\mathbf{r}; R) , \quad (4.7)$$

where we are working in the MOL frame where the z -axis is aligned with the molecular axis. Cylindrical symmetry then implies $\langle p^x p^x \rangle = \langle p^y p^y \rangle$, while $\langle p^a p^b \rangle$ vanishes for $a \neq b$. With $\gamma(R)$ set to 1, we find the analytic expressions

$$\langle p^x p^x \rangle_1 = \langle p^y p^y \rangle_1 = \frac{1}{3(1 + I_0)} (1 + (1 + R)e^{-R}) , \quad (4.8)$$

and

$$\langle p^z p^z \rangle_1 = \frac{1}{3} \frac{1}{(1 + I_0)} (1 + (1 + R - R^2)e^{-R}) . \quad (4.9)$$

Reinstating $\gamma(R)$, in this case we have

$$\langle p^a p^b \rangle_\gamma(R) = \gamma(R)^2 \langle p^a p^b \rangle_1(\gamma(R)R) . \quad (4.10)$$

These momentum expectation values are plotted in Fig. 2 (see also Fig. 5 in Appendix A). Since full spherical symmetry is restored as both $R \rightarrow 0$ and $R \rightarrow \infty$, we expect all three expectation values to be equal in these limits and related in the obvious way to the kinetic energy, implying (no sum on a) $\langle p^a p^a \rangle \rightarrow 4/3$ as $R \rightarrow 0$ and $\langle p^a p^a \rangle \rightarrow 1/3$ for large R . This is confirmed in the explicit numerical solutions.

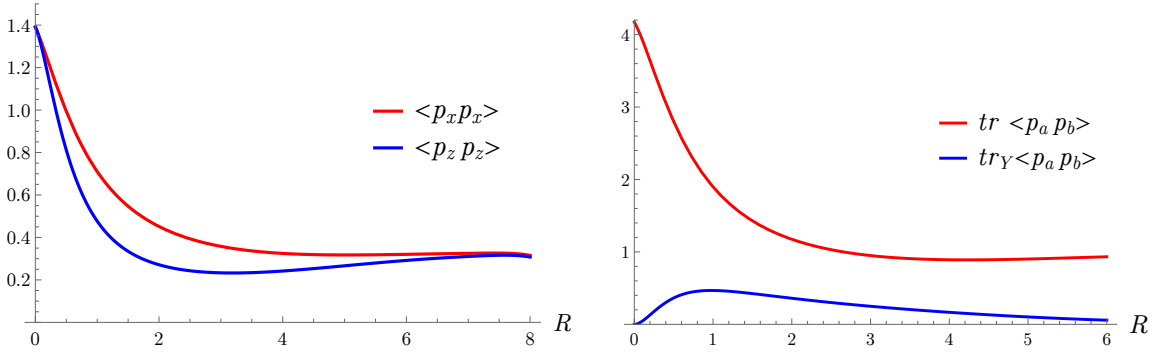


Figure 2. The momentum expectation values which determine the Lorentz and CPT violating contributions to the nucleon Schrödinger equation arising from the SME couplings of the electron as a function of the bond length R . The left hand figure shows $\langle p^x p^x \rangle$ (red, upper) and $\langle p^z p^z \rangle$ (blue) evaluated with the scaling factor $\gamma(R)$. The right hand figure is the same for $\text{tr} \langle p^a p^b \rangle$ (red) and $\text{tr}_Y \langle p^a p^b \rangle$ (blue) defined below.

Next, since these momentum expectation values are evaluated in the MOL frame whereas we want to express the rovibrational energies in terms of the Lorentz and CPT couplings \tilde{E}_{ij} in the EXP frame, we need to find the relation between these frames.

The rotation matrix relating the EXP and MOL basis vectors, where $\mathbf{e}_i = \mathbf{e}_a R_{ai}$, is⁶

$$R_{ai} = \begin{pmatrix} \cos \theta \cos \phi & \cos \theta \sin \phi & -\sin \theta \\ -\sin \phi & \cos \phi & 0 \\ \sin \theta \cos \phi & \sin \theta \sin \phi & \cos \theta \end{pmatrix} . \quad (4.11)$$

⁶To transform from the MOL to the EXP frame we use the usual Euler angles, noting that only two of the three required in general are necessary here because of the cylindrical symmetry in the MOL frame of reference. Then R_{ai} comprises (i) a rotation of $-\theta$ about the MOL y -axis, followed by (ii) a

The angles (θ, ϕ) here are the standard spherical polar coordinates specifying the orientation of the molecular axis in the EXP frame.

The SME couplings are then related by

$$\tilde{E}_{ab}^e = R_{ai} \tilde{E}_{ij}^e (R^\top)_{jb} . \quad (4.12)$$

The SME potential $V_{\text{SME}}^e(\mathbf{R}) \equiv V_{\text{SME}}^e(R, \theta, \phi)$ in (3.5) is therefore

$$\begin{aligned} V_{\text{SME}}^e(R, \theta, \phi) &= \frac{1}{m_e^2} \langle p^a p^b \rangle \tilde{E}_{ab}^e \\ &= \frac{1}{m_e^2} \langle p^a p^b \rangle R_{ai} \tilde{E}_{ij}^e (R^\top)_{jb} \end{aligned} \quad (4.13)$$

and using the cylindrical symmetry to set $\langle p^y p^y \rangle = \langle p^x p^x \rangle$, we can rewrite this as

$$V_{\text{SME}}^e(R, \theta, \phi) = \frac{1}{m_e^2} \left[\langle p^x p^x \rangle \delta_{ij} + (\langle p^z p^z \rangle - \langle p^x p^x \rangle) (R^\top)_{iz} R_{zj} \right] \tilde{E}_{ij}^e . \quad (4.14)$$

This greatly simplifies the calculation, since we now only need to evaluate the symmetric matrix

$$(R^\top)_{iz} R_{zj} = \begin{pmatrix} \sin^2 \theta \cos^2 \phi & \frac{1}{2} \sin^2 \theta \sin 2\phi & \frac{1}{2} \sin 2\theta \cos \phi \\ \dots & \sin^2 \theta \sin^2 \phi & \frac{1}{2} \sin 2\theta \sin \phi \\ \dots & \dots & \cos^2 \theta \end{pmatrix} . \quad (4.15)$$

The final step to derive the potential $V_{\text{SME}}^e(R)$ to be used in the nucleon Schrödinger equation (3.6) is to take the expectation value in (3.7), *viz.*

$$V_{\text{SME}}^e(R) = \int d\Omega Y_{NM_N}^*(\theta, \phi) V_{\text{SME}}^e(R, \theta, \phi) Y_{NM_N}(\theta, \phi) . \quad (4.16)$$

Notice that this assumes the states are eigenstates of both N and M_N . This will not necessarily be the case when we consider the hyperfine-Zeeman spectrum, which we discuss in detail in Paper 2 [20].

rotation of $-\phi$ about the new MOL z -axis, that is

$$R_{ai} = \begin{pmatrix} \cos \theta & 0 & -\sin \theta \\ 0 & 1 & 0 \\ \sin \theta & 0 & \cos \theta \end{pmatrix} \begin{pmatrix} \cos \phi & \sin \phi & 0 \\ -\sin \phi & \cos \phi & 0 \\ 0 & 0 & 1 \end{pmatrix} .$$

To evaluate (4.16), first expand $(R^\top)_{iz} R_{zj}$ in terms of spherical harmonics as

$$(R^\top)_{iz} R_{zj} = \sum_M C_{ij}^M Y_{2M}(\theta, \phi) + \tilde{C}_{ij}^0 Y_{00} , \quad (4.17)$$

with

$$C_{ij}^M = \int d\Omega (R^\top)_{iz} R_{zj} Y_{2M}(\theta, \phi) . \quad (4.18)$$

The combination $\tilde{C}_{ij}^0 Y_{00} = 1/3 \delta_{ij}$ follows without further calculation by noting that $\text{tr}(R^\top)_{iz} R_{zj} = 1$ and $\text{tr} C_{ij}^M = 0$. In fact, we only need to calculate C_{ij}^M for $M = 0$, and with standard normalisations of the spherical harmonics we readily find [25],

$$C_{ij}^0 = -\frac{2}{3} \sqrt{\frac{\pi}{5}} \begin{pmatrix} 1 & 0 & 0 \\ 0 & 1 & 0 \\ 0 & 0 & -2 \end{pmatrix} . \quad (4.19)$$

The expectation value (4.16) is evaluated in terms of Clebsch-Gordan coefficients using the Gaunt integral,

$$\int d\Omega Y_{NM_N}^*(\theta, \phi) Y_{2M}(\theta, \phi) Y_{NM_N}(\theta, \phi) = \frac{1}{2} \sqrt{\frac{5}{\pi}} C_{NM_N;20}^{NM_N} C_{N0;20}^{N0} \delta_{M0} , \quad (4.20)$$

and we find

$$\begin{aligned} V_{\text{SME}}^e(R) = & \frac{1}{m_e^2} \left[\langle p^x p^x \rangle \delta_{ij} \right. \\ & \left. + (\langle p^z p^z \rangle - \langle p^x p^x \rangle) \left(\frac{1}{2} \sqrt{\frac{5}{\pi}} C_{NM_N;20}^{NM_N} C_{N0;20}^{N0} C_{ij}^0 + \frac{1}{3} \delta_{ij} \right) \right] \tilde{E}_{ij}^e . \end{aligned} \quad (4.21)$$

The Clebsch-Gordan coefficients are known analytically, and simplifying we have

$$C_{NM_N;20}^{NM_N} C_{N0;20}^{N0} = \frac{N(N+1) - 3M_N^2}{(2N-1)(2N+3)} \equiv c_{NM_N} , \quad (4.22)$$

which vanishes for $N = 0$. Collecting these results and rearranging, we therefore find our final result for the Lorentz and CPT violating contribution $V_{\text{SME}}^e(R)$ to the inter-nucleon potential [11],

$$\begin{aligned} V_{\text{SME}}^e(R) = & \frac{1}{3} \frac{1}{m_e^2} \left[(2\langle p^x p^x \rangle + \langle p^z p^z \rangle) \text{tr} \tilde{E}_{ij}^e \right. \\ & \left. + (\langle p^x p^x \rangle - \langle p^z p^z \rangle) c_{NM_N} \text{tr}_Y \tilde{E}_{ij}^e \right] , \end{aligned} \quad (4.23)$$

where we define $\text{tr}_Y \tilde{E}_{ij} = \tilde{E}_{11} + \tilde{E}_{22} - 2\tilde{E}_{33}$. As anticipated, the Lorentz and CPT violating couplings introduce an explicit M_N dependence in $V_{\text{SME}}^e(R)$ ⁷ ultimately breaking the degeneracy of the nucleon rovibrational levels with fixed v, N .

5 Rovibrational energy levels

We now move on to an explicit derivation of the rovibrational energy levels for the (anti-)hydrogen molecular ion, first without Lorentz and CPT violation and then incorporating the breaking potential $V_{\text{SME}}^e(R)$. We work analytically throughout, quoting our final answers in terms of derivatives of $V_M(R)$ and $V_{\text{SME}}^e(R)$ with respect to the inter-nucleon separation R , the latter being governed by the derivatives of the momentum expectation values in (4.21). Numerical estimates for these derivatives have been calculated in Appendix A, but we delay using these to keep maximum generality for as long as possible. An alternative approach, potentially more systematic, to calculating the rovibrational levels is given in Appendix B. Both approaches bring different physical insights into the physical origin of the various contributions to the energy levels.

We now pick up the discussion from the end of section 2. The first objective is to calculate the coefficients x_0, B_0, α_0 and D_0 in the theory with no Lorentz or CPT violation. We start by including the angular momentum term in the nucleon Schrödinger equation (2.9) in an *effective* potential $V_{\text{eff}}(R)$ and study the simple harmonic motion about the minimum of this potential. So we define

$$V_{\text{eff}}(R) = V_M(R) + \frac{1}{2\mu R^2} N(N+1). \quad (5.1)$$

The angular momentum term changes the mean inter-nucleon separation (bond length) and the vibration frequency perturbatively in the small parameter $\lambda = 1/(\mu \omega_0 R_0^2)$ that was introduced in section 2.

First, let $R_m = R_0 + \delta R$ be the minimum of the effective potential. Setting $V'_{\text{eff}}(R_m) = 0$, we find

$$\frac{\delta R}{R_0} = \lambda^2 N(N+1) - \left(3 + \frac{1}{2} \frac{R_0 V_M'''(R_0)}{V_M''(R_0)}\right) \lambda^4 (N(N+1))^2 + \dots \quad (5.2)$$

⁷Logically, we should display the N, M_N dependence explicitly by writing $V_{\text{SME};NM_N}^e(R)$ as we do for the energy eigenvalues E_{vNM_N} but this notation becomes cumbersome and we suppress these labels in what follows.

The corresponding shift in the bond length is interpreted as “centrifugal stretching” as the centrifugal force due to the orbital angular momentum stretches the effective spring binding the nucleons.

Evaluating the effective potential at the new minimum gives

$$\begin{aligned} V_{eff}(R_m) &= V_{eff}(R_0) + \delta R V'_{eff}(R_0) + \frac{1}{2} \delta R^2 V''_{eff}(R_0) + \dots \\ &= V_M(R_0) + \frac{1}{2} \lambda N(N+1) \omega_0 - \frac{1}{2} \lambda^3 (N(N+1))^2 \omega_0 + \dots \end{aligned} \quad (5.3)$$

The coefficient of this $O(N(N+1))^2$ term is of importance later. It arises here as a combination of two terms, one with a pre-factor -1 from the $O(\delta R)$ contribution, where it is interpreted as reduced *kinetic* energy due to centrifugal stretching at fixed N , and one with pre-factor $1/2$ from the $O(\delta R)^2$ contribution which is interpreted as the extra *potential* energy due to this stretching of the inter-nucleon bond.

Next, we need the change in the effective vibrational frequency due to expanding about the minimum of $V_{eff}(R)$. Here,

$$\begin{aligned} V''_{eff}(R_m) &= V''_{eff}(R_0) + \delta R V'''_{eff}(R_0) + \dots \\ &= V''_M(R_0) \left[1 + \left(3 + \frac{R_0 V'''_M(R_0)}{V''_M(R_0)} \right) \lambda^2 N(N+1) + O(\lambda^4 (N(N+1))^2) \right]. \end{aligned} \quad (5.4)$$

We have also calculated the $O(\lambda^4 (N(N+1))^2)$ term here, which has a coefficient involving up to four derivatives of the potential $V_M(R)$. These lead to contributions to the rovibrational energy (2.10) of $O((v + \frac{1}{2})(N(N+1))^2)$, which are obviously very small and are omitted in this paper for simplicity.

The new oscillation frequency ω is then

$$\omega = \omega_0 \left[1 + \frac{1}{2} \left(3 + \frac{R_0 V'''_M(R_0)}{V''_M(R_0)} \right) \lambda^2 N(N+1) + \dots \right], \quad (5.5)$$

with a corresponding contribution $(v + \frac{1}{2})\omega$ to the energy.

The term proportional to $V'''_M(R_0)$ in (5.5), which contributes to the coefficient α_0 below, has an interesting interpretation in terms of “vibrational stretching” of the bond length in the presence of an asymmetric potential. In particular, in the case of an anharmonic oscillator with a cubic interaction, the expectation value of the position is

shifted from the minimum of the potential.⁸ Applying this result to the expansion of the angular momentum term $V_N(R)$ in (5.1),

$$V_N(R) = \frac{1}{2}\lambda\omega_0 N(N+1) \left(1 - 2\frac{\langle x \rangle}{R_0} + \dots\right), \quad (5.6)$$

where we write $R = R_0 + x$, and evaluating $\langle x \rangle$ approximating $V_M(R)$ as an anharmonic oscillator, we have

$$\frac{\langle x \rangle}{R_0} = -\frac{1}{2}\lambda \frac{R_0 V_M'''(R_0)}{V_M''(R_0)} \left(v + \frac{1}{2}\right), \quad (5.7)$$

which reproduces the equivalent term in the energy found through the alternative route in (5.5). This derivation makes clear that this is an increase in *kinetic* energy at fixed N due to the reduction in mean bond length from (5.7).

Finally, collecting all these results, we find the coefficients in the expansion

$$\begin{aligned} E_{vN} = & (v + \frac{1}{2})\omega_0 - x_0 (v + \frac{1}{2})^2 \omega_0 \\ & + B_0 N(N+1)\omega_0 - \alpha_0 (v + \frac{1}{2})N(N+1)\omega_0 - D_0 (N(N+1))^2 \omega_0 + \dots \end{aligned} \quad (5.8)$$

of the rovibrational energies are

$$\begin{aligned} B_0 = \frac{1}{2}\lambda, \quad \alpha_0 = -\frac{1}{2}\left(3 + \frac{R_0 V_M'''}{V_M''}\right)\lambda^2, \\ D_0 = \frac{1}{2}\lambda^3, \quad x_0 = \left[\frac{5}{48}\left(\frac{R_0 V_M'''}{V_M''}\right)^2 - \frac{1}{16}\left(\frac{R_0^2 V_M^{(4)}}{V_M''}\right)\right]\lambda, \end{aligned} \quad (5.9)$$

where all the indicated derivatives of $V_M(R)$ are taken at R_0 .

The result for x_0 arises from taking into account the anharmonic nature of the potential and including the $O(v + \frac{1}{2})^2$ contributions to the energy of an anharmonic oscillator with a $gx^3 + hx^4$ potential, where we identify $g = \frac{1}{6}V_M'''$ and $h = \frac{1}{24}V_M^{(4)}$. These are proportional to h at first order and g^2 at second order. The explicit formulae, which determine x_0 in (5.9), are quoted in footnote 9.

⁸Consider an anharmonic oscillator with potential $V(x) = \frac{1}{2}\mu\omega_0^2 x^2 + gx^3$. The expectation value $\langle x \rangle$ evaluated in the unperturbed SHO states gives

$$\langle x \rangle = -g \frac{3}{\mu^2 \omega_0^3} \left(v + \frac{1}{2}\right).$$

Notice that the sign of $\langle x \rangle$ is opposite to the sign of the cubic anharmonic term in the potential.

Importantly, each quoted coefficient is the leading term in an expansion in λ . At each order, the prefactors are known numbers involving successively higher derivatives of the basic inter-nucleon potential. We have derived these in Appendix A to a precision sufficient for our purpose here, which is to determine the leading corrections to (5.8) when Lorentz and CPT violating interactions are introduced.

We now need to extend this calculation to include the Lorentz and CPT violating potential $V_{\text{SME}}^e(R)$ in the nucleon Schrödinger equation. The idea is to iterate the effective potential method for the hierarchy of perturbations, first including only the angular momentum term as above, then including the potential $V_{\text{SME}}^e(R)$ as a further small perturbation. As always, the Lorentz and CPT perturbations are considered the smallest, and we work only to first order in the SME couplings so terms of $O(V_{\text{SME}}^e)^2$ are immediately dropped.

So here we define

$$U_{\text{eff}}(R) = V_{\text{eff}}(R) + V_{\text{SME}}^e(R) , \quad (5.10)$$

and expand about the minimum R_u of $U_{\text{eff}}(R)$. Setting $U'_{\text{eff}}(R_u) = 0$ with $R_u = R_m + \delta R_u$, we have

$$\frac{\delta R_u}{R_m} = -\frac{1}{R_m V''_{\text{eff}}(R_m)} V_{\text{SME}}^{e'}(R_m) . \quad (5.11)$$

We then find, repeating the steps (5.3) and (5.4) above and neglecting terms of $O(\text{SME})^2$, that

$$\begin{aligned} U_{\text{eff}}(R_u) &= U_{\text{eff}}(R_m) + \delta R_u U'_{\text{eff}}(R_m) \\ &= V_{\text{eff}}(R_m) + V_{\text{SME}}^e(R_m) , \end{aligned} \quad (5.12)$$

and

$$U''_{\text{eff}}(R_u) = V''_{\text{eff}}(R_m) + V_{\text{SME}}^{e''}(R_m) - \frac{V'''_{\text{eff}}(R_m)}{V''_{\text{eff}}(R_m)} V_{\text{SME}}^{e'}(R_m) , \quad (5.13)$$

the latter giving the new effective vibration frequency ω_u .

The next step is to rewrite (5.12) and (5.13) in terms of derivatives at the minimum R_0 of the original potential $V_M(R)$, rather than at R_m . We have already found $V_{\text{eff}}(R_m)$

and $V_{\text{eff}}''(R_m)$ in (5.3) and (5.4), so we just need

$$\begin{aligned}
U_{\text{eff}}(R_u) &= V_{\text{eff}}(R_m) + V_{\text{SME}}^e(R_0) + \delta R V_{\text{SME}}^{e'}(R_0) + \frac{1}{2} \delta R^2 V_{\text{SME}}^{e''}(R_0) \\
&= V_{\text{eff}}(R_m) + V_{\text{SME}}^e(R_0) \\
&\quad + \left[\lambda^2 N(N+1) - \left(3 + \frac{1}{2} \frac{R_0 V_M'''}{V_M''} \right) \lambda^4 (N(N+1))^2 \right] R_0 V_{\text{SME}}^{e'}(R_0) \\
&\quad + \frac{1}{2} \lambda^4 (N(N+1))^2 R_0^2 V_{\text{SME}}^{e''}(R_0) , \tag{5.14}
\end{aligned}$$

which gives the Lorentz and CPT violating contributions B_{SME}^e and D_{SME}^e in (5.17) below, then from (5.13), and after some lengthy but straightforward algebra, we find

$$\begin{aligned}
U_{\text{eff}}''(R_u) &= V_{\text{eff}}''(R_m) + V_{\text{SME}}^{e''}(R_0) - \frac{V_M'''}{V_M''} V_{\text{SME}}^{e'}(R_0) \\
&\quad + \lambda^2 N(N+1) \left[R_0 V_{\text{SME}}^{e'''}(R_0) - \frac{V_M'''}{V_M''} \left(R_0 V_{\text{SME}}^{e''}(R_0) + \beta V_{\text{SME}}^{e'}(R_0) \right) \right] , \tag{5.15}
\end{aligned}$$

again with the understanding that all derivatives of V_M are taken at R_0 . Here,

$$\beta = 3 - 12 \frac{V_M'''}{R_0 V_M''} - \frac{R_0 V_M'''}{V_M''} + \frac{R_0 V_M^{(4)}}{V_M'''} . \tag{5.16}$$

The new effective vibration frequency is now given by $\omega_u^2 = \omega_0^2 U_{\text{eff}}''(R_0)/V_M''(R_0)$ and the corresponding energy levels by $(v + \frac{1}{2})\omega_u$. This gives contributions to α_{SME}^e and δ_{SME}^e , defined below.

The Lorentz and CPT corrections to the rovibrational energies (5.8) can therefore be written in the form

$$\begin{aligned}
E_{vNMN} &= V_{\text{SME}}^e + (1 + \delta_{\text{SME}}^e) (v + \frac{1}{2}) \omega_0 - (x_0 + x_{\text{SME}}^e) (v + \frac{1}{2})^2 \omega_0 \\
&\quad + (B_0 + B_{\text{SME}}^e) N(N+1) \omega_0 - (\alpha_0 + \alpha_{\text{SME}}^e) (v + \frac{1}{2}) N(N+1) \omega_0 \\
&\quad - (D_0 + D_{\text{SME}}^e) (N(N+1))^2 \omega_0 + \dots \tag{5.17}
\end{aligned}$$

with $V_{\text{SME}}^e \equiv V_{\text{SME}}^e(R_0)$ and coefficients,

$$\begin{aligned}
\delta_{\text{SME}}^e &= \frac{1}{2} \frac{1}{V_M''} \left[V_{\text{SME}}^{e''} - \frac{V_M'''}{V_M''} V_{\text{SME}}^{e'} \right] \\
B_{\text{SME}}^e &= \lambda \frac{1}{V_M''} \left[\frac{1}{R_0} V_{\text{SME}}^{e'} \right] \\
\alpha_{\text{SME}}^e &= \lambda^2 \frac{1}{V_M''} \left[-\frac{1}{2} R_0 V_{\text{SME}}^{e'''} + \frac{3}{4} \left(1 + \frac{R_0 V_M'''}{V_M''} \right) V_{\text{SME}}^{e''} \right. \\
&\quad \left. - \left(6 + \frac{9}{4} \frac{R_0 V_M'''}{V_M''} + \frac{3}{4} \left(\frac{R_0 V_M'''}{V_M''} \right)^2 - \frac{1}{2} \frac{R_0^2 V_M^{(4)}}{V_M''} \right) \frac{1}{R_0} V_{\text{SME}}^{e'} \right] \\
D_{\text{SME}}^e &= \lambda^3 \frac{1}{V_M''} \left[-\frac{1}{2} V_{\text{SME}}^{e''} + \left(3 + \frac{1}{2} \frac{R_0 V_M'''}{V_M''} \right) \frac{1}{R_0} V_{\text{SME}}^{e'} \right]. \tag{5.18}
\end{aligned}$$

Notice that the ω_0 -independent term V_{SME}^e should be retained here since it depends on the quantum numbers N, M_N through (4.23) and so contributes to rovibrational transition energies in which $\Delta N \neq 0$.

The final coefficient x_{SME}^e is found from the anharmonic terms as before, where here $g = \frac{1}{6} U_{\text{eff}}'''(R_u)$ and $h = \frac{1}{24} U_{\text{eff}}^{(4)}(R_u)$. Since we are not calculating terms involving the angular momentum at $O(v + \frac{1}{2})^2$, we may simplify $U_{\text{eff}}(R)$ in (5.10) to be just $V_M(R) + V_{\text{SME}}^e(R)$, with the corresponding simplification of δR_u in (5.11). Then we use the AHO energies in footnote⁹ to extract x_{SME}^e , keeping terms of first order in the SME couplings only. There are two sources of extra terms beyond the simple extension of x_0 in (5.9). The first comes from writing the derivatives at R_0 rather than R_u ; thus, for example, $U_{\text{eff}}^{(4)}(R_u) \rightarrow V_M^{(4)}(R_0) + V_{\text{SME}}^{e(4)}(R_0) + \delta R_u V_M^{(5)}(R_0)$, which produces extra terms proportional to $V_{\text{SME}}^{e'}$. Next, we must remember that the frequency in the AHO energies is now ω_u not ω_0 , where $\mu \omega_u^2 = U_{\text{eff}}''(R_u)$ in (5.15). Including both corrections

⁹Explicitly, for an anharmonic oscillator with potential $V = \frac{1}{2} \mu \omega_0^2 x^2 + gx^3 + hx^4$, and working to 2nd order perturbation theory in g , the kinetic energy $K = p^2/2\mu$ is

$$\begin{aligned}
\langle K \rangle &= \frac{1}{2} (v + \frac{1}{2}) \omega_0 + \frac{3}{2} \frac{h}{\mu^2 \omega_0^3} \left((v + \frac{1}{2})^2 + \frac{1}{4} \right) \omega_0 - \frac{1}{16} \frac{g^2}{\mu^3 \omega_0^5} (60(v + \frac{1}{2})^2 + 7) \omega_0 \\
&= \frac{1}{2} E_v^{(0)} + E_v^{(1)}(\lambda) + E_v^{(2)}(g^2),
\end{aligned}$$

where E_v are the total energies at the indicated order.

eventually gives

$$x_{\text{SME}}^e = \lambda \frac{1}{V_M''} \left[\frac{5}{24} R_0^2 \frac{V_M'''}{V_M''} \left(V_{\text{SME}}^{e'''} - \frac{V_M'''}{V_M''} V_{\text{SME}}^{e''} + \left(\left(\frac{V_M'''}{V_M''} \right)^2 - \frac{V_M^{(4)}}{V_M''} \right) V_{\text{SME}}^{e'} \right) \right. \\ \left. - \frac{1}{16} R_0^2 \left(V_{\text{SME}}^{e(4)} - \frac{V_M^{(4)}}{V_M''} V_{\text{SME}}^{e''} + \left(\frac{V_M'''}{V_M''} \frac{V_M^{(4)}}{V_M''} - \frac{V_M^{(5)}}{V_M''} \right) V_{\text{SME}}^{e'} \right) \right]. \quad (5.19)$$

We should perhaps emphasise that while these expressions appear complicated, the coefficients of V_{SME}^e and its derivatives are just simple numerical factors determined by $V_M(R)$ and have been evaluated in Appendix A. That said, *all* the V_M -dependent terms shown in these coefficients are necessary, since there is no reason to discard those with higher derivatives of V_M as being smaller. As a check that the effective potential method used here has indeed correctly and completely identified all the terms occurring at the required order in λ , we present an alternative, especially systematic, perturbative method of evaluation in Appendix B.

At this point, in addition to the rovibrational energies themselves, we can deduce expressions for the Lorentz and CPT violating effects on the mean inter-nucleon bond length and the dissociation energy.

As well as the N -dependent centrifugal stretching, the mean bond length is also affected by the SME couplings. This contribution, ΔR_{SME} , is simply identified in the effective potential method as δR_u in (5.11). Expanding the potentials $V_{\text{SME}}^{e'}(R_m)$ and $V_{\text{eff}}''(R_m)$ about R_0 instead of R_m , we find

$$\Delta R_{\text{SME}} = -\frac{1}{V_M''} \left[V_{\text{SME}}^{e'} + \lambda^2 N(N+1) \left(R_0 V_{\text{SME}}^{e''} - \left(3 + \frac{R_0 V_M'''}{V_M''} \right) V_{\text{SME}}^{e'} \right) \right], \quad (5.20)$$

up to higher order terms of $O(\lambda^2 N(N+1))^2$.

We define the dissociation energy E^{diss} as the difference between the energy of the ground state and the value of the inter-nucleon potential in the large- R limit. The SME correction to the dissociation energy is then,

$$\Delta E_{\text{SME}}^{\text{diss}} = V_{\text{SME}}^e(\infty) - V_{\text{SME}}^e(R_0) - \frac{1}{2} \delta_{\text{SME}}^e \omega_0. \quad (5.21)$$

This is evaluated explicitly in the following section, noting that since $\langle p^a p^b \rangle \rightarrow (1/3)\delta^{ab}$ as $R \rightarrow \infty$, reflecting the spherical symmetry in this limit, the second term in (4.23) for $V_{\text{SME}}^e(\infty)$ vanishes.

The remaining contribution to the rovibrational energies comes from the direct contribution ΔE_{SME}^n from the Lorentz and CPT violating proton couplings E_{ij}^p in the nucleon Schrödinger equation. Recall from (3.8) that this requires us to evaluate the expectation value

$$\Delta E_{\text{SME}}^n = \frac{2}{m_p^2} E_{ij}^p \langle v N M_N | P^i P^j | v N M_N \rangle , \quad (5.22)$$

in the original nucleon states $|v N M_N\rangle$, with all quantities expressed in the EXP frame. The analysis mirrors that described in detail in section 4. First, we expand $P^i P^j$ in spherical harmonics,

$$P_i P_j = P^2 \left(\frac{1}{3} \delta_{ij} + \sum_M C_{ij}^M Y_{2M}(\theta, \phi) \right) , \quad (5.23)$$

where (θ, ϕ) are the spherical polar angles made by the molecular axis (and therefore \mathbf{P}) in the EXP frame, *i.e.* $P_i = |\mathbf{P}|(\sin \theta \cos \phi, \sin \theta \sin \phi, \cos \theta)$. Noting then that $P_i P_j = P^2 (R^T)_{iz} R_{zj}$, which of course is inherent in the construction of (4.15), the coefficient C_{ij}^M here is identical to that found in section 4. Taking the expectation value as in (4.20) and evaluating the Clebsch-Gordan equations (4.22), we find without further calculation that

$$\Delta E_{\text{SME}}^n = \langle v N | P^2 | v N \rangle \frac{2}{m_p^2} \left[\frac{1}{3} \text{tr} E_{ij}^p - \frac{1}{3} c_{NM_N} \text{tr}_Y E_{ij}^p \right] \quad (5.24)$$

The problem therefore reduces to finding the expectation value $\langle P^2 \rangle$ of the nucleon momentum. In this case, we do not have a simple explicit wave function solving the Schrödinger equation, so a direct evaluation is not straightforward. However, since $P^2/2\mu$ is just the kinetic energy, all we need in practice is to identify the kinetic energy part of the total rovibrational energy E_{vN} in (5.8). This requires examining each of the coefficients x_0, B_0, α_0 and D_0 derived above and deducing on physical grounds what is their *kinetic* energy component.

First, write (5.24) as

$$\Delta E_{\text{SME}}^n = \langle v N | K | v N \rangle \tilde{V}_{\text{SME}}^n , \quad (5.25)$$

with

$$\tilde{V}_{\text{SME}}^n = \frac{2}{3} \frac{1}{m_p} \left[\text{tr} E_{ij}^p - c_{NM_N} \text{tr}_Y E_{ij}^p \right] . \quad (5.26)$$

Then, adding this contribution to (5.17), the rovibrational energies including all the Lorentz and CPT breaking contributions are written as

$$\begin{aligned}
E_{vNMN} &= V_{\text{SME}}^e + (1 + \delta_{\text{SME}}^e + \delta_{\text{SME}}^n) (v + \frac{1}{2}) \omega_0 - (x_0 + x_{\text{SME}}^e + x_{\text{SME}}^n) (v + \frac{1}{2})^2 \omega_0 \\
&+ (B_0 + B_{\text{SME}}^e + B_{\text{SME}}^n) N(N + 1) \omega_0 \\
&- (\alpha_0 + \alpha_{\text{SME}}^e + \alpha_{\text{SME}}^n) (v + \frac{1}{2}) N(N + 1) \omega_0 \\
&- (D_0 + D_{\text{SME}}^e + D_{\text{SME}}^n) (N(N + 1))^2 \omega_0 + \dots
\end{aligned} \tag{5.27}$$

Beginning with the angular momentum independent terms, x_0 is found to $O(\lambda)$ by approximating $V_M(R)$ as an anharmonic oscillator with cubic and quartic interactions. An explicit calculation, consistent with the virial theorem, shows that at $O(v + 1/2)$ the kinetic energy is $E_v/2$ while at $O(v + 1/2)^2$ the whole energy is kinetic (see footnote 9). It follows immediately that the corresponding coefficients in (5.27) are

$$\delta_{\text{SME}}^n = \frac{1}{2} \tilde{V}_{\text{SME}}^n, \quad x_{\text{SME}}^n = x_0 \tilde{V}_{\text{SME}}^n. \tag{5.28}$$

Turning to the N -dependent terms, it is clear that B_0 is a pure kinetic energy term. However, For D_0 we emphasised above there were two contributions, weighted -1 and 1/2, which arose due to centrifugal stretching. Of these the first represents a reduction in kinetic energy, while the second is potential energy due to stretching the mean bond length. This means we must take

$$B_{\text{SME}}^n = B_0 \tilde{V}_{\text{SME}}^n, \quad D_{\text{SME}}^n = 2 D_0 \tilde{V}_{\text{SME}}^n. \tag{5.29}$$

For α_{SME}^n , an interpretation based on the effective potential is less clear, but a careful analysis using the methods in Appendix B shows that it follows the same pattern as above, and we have

$$\alpha_{\text{SME}}^n = \frac{3}{2} \alpha_0 \tilde{V}_{\text{SME}}^n. \tag{5.30}$$

Together, (5.26) to (5.30) complete the derivation of the Lorentz and CPT violating contributions to the rovibrational energy levels.

6 The rovibrational spectrum

In this section, we draw together all the results of sections 4 and 5 and the appendices to describe the implications of Lorentz and CPT violation for the rovibrational spectrum of the (anti-)hydrogen molecular ion.

First, we verify that our approximate methods describe the rovibrational spectrum in the absence of Lorentz and CPT symmetry breaking sufficiently for our objective, that is to constrain the SME couplings with greater precision than is possible with atomic (anti-)hydrogen alone. For this, we need the numerical results for $V_M(R)$ and its derivatives tabulated in Appendix A, Table 1. The key result is for the vibrational angular frequency ω_0 . Converting from the atomic units of Table 1 using $\hat{R}_H = 1/(2\hat{\mu}\hat{a}_0^2)$, we find (with $\hbar = c = 1$),

$$\omega_0 = \sqrt{\frac{2V_M''(R_0)}{m_p}} = 0.020 \hat{R}_H = 0.275 \text{ eV} , \quad (6.1)$$

which in terms of the fundamental QED parameters implies $w_0 \sim R_H \sqrt{\frac{m_e}{m_p}}$. In standard spectroscopic units (with $h = c = 1$), $1 \text{ eV} = 2.418 \times 10^{14} \text{ Hz} = 8065.5 \text{ cm}^{-1}$, so the corresponding frequency is 2218 cm^{-1} .

The dimensionless expansion parameter λ is then determined for the H_2^+ ion as $\lambda = 1/(\mu\omega_0 R_0^2) = 0.027$. Note that this is parametrically $\lambda \sim \sqrt{\frac{m_e}{m_p}}$.

The coefficients of the expansion (5.8) of the rovibrational energy levels,

$$\begin{aligned} E_{vN} = & (v + \tfrac{1}{2})\omega_0 - x_0(v + \tfrac{1}{2})^2\omega_0 \\ & + B_0 N(N+1)\omega_0 - \alpha_0(v + \tfrac{1}{2})N(N+1)\omega_0 - D_0(N(N+1))^2\omega_0 + \dots \end{aligned} \quad (6.2)$$

are then found from Table 1 to be

$$\begin{aligned} B_0 = \frac{1}{2}\lambda = 0.0135 , & \quad \alpha_0 = 1.133\lambda^2 = 0.819 \times 10^{-3} , \\ D_0 = \frac{1}{2}\lambda^3 = 1.944 \times 10^{-5} & \quad x_0 = 1.230\lambda = 0.033 . \end{aligned} \quad (6.3)$$

Substituting back, we find the rovibrational levels in spectroscopic units of cm^{-1} in the form,

$$\begin{aligned} E_{vN} = & 2218(v + \tfrac{1}{2}) - 73.2(v + \tfrac{1}{2})^2 \\ & + 29.82 N(N+1) - 1.82(v + \tfrac{1}{2})N(N+1) - 0.0216(N(N+1))^2 + \dots \end{aligned} \quad (6.4)$$

which may be compared with precision calculations and data.¹⁰ The hierarchy of the coefficients in powers of λ is immediately evident. A particular point of interest already here is that the term in (5.9) involving the third derivative V_M''' is essential even to give the correct sign for the $O(v + \frac{1}{2}) N(N + 1)$ contribution. Moreover, the x_0 coefficient, which is determined entirely by the higher derivative terms in $V_M(R)$, has the correct value and sign to produce the narrowing of vibrational energy level splittings as v becomes larger, allowing roughly 20 vibrational states below the dissociation energy. Both these observations confirm the necessity of including a full analysis of the anharmonic terms in $V_M(R)$ to produce a realistic match to the rovibrational spectrum and ensure our results remain valid beyond the lowest vibrational states.

We now turn to the Lorentz and CPT violating effects in the rovibrational spectrum. Writing the coefficients δ_{SME}^e , B_{SME}^e, \dots in (5.18), (5.19) in terms of V_{SME}^e and its derivatives using the numerical values in Table 1 gives, in atomic units,

$$\begin{aligned}
\delta_{\text{SME}}^e &= [2.669 V_{\text{SME}}^{e''} + 7.018 V_{\text{SME}}^{e'}] \\
B_{\text{SME}}^e &= \lambda [2.664 V_{\text{SME}}^{e'}] \\
\alpha_{\text{SME}}^e &= \lambda^2 [-5.346 V_{\text{SME}}^{e'''} - 17.084 V_{\text{SME}}^{e''} - 3.408 V_{\text{SME}}^{e'}] \\
D_{\text{SME}}^e &= \lambda^3 [-2.669 V_{\text{SME}}^{e''} + 0.897 V_{\text{SME}}^{e'}] \\
x_{\text{SME}}^e &= \lambda [-1.337 V_{\text{SME}}^{e(4)} - 11.738 V_{\text{SME}}^{e'''} - 22.004 V_{\text{SME}}^{e''} - 5.215 V_{\text{SME}}^{e'}] . \quad (6.5)
\end{aligned}$$

The next step is to re-express V_{SME}^e in (4.23) in atomic units, as assumed here. Recalling $R_H = 1/(2 m_e a_0^2)$,¹¹ we write $V_{\text{SME}}^e(R)$ as

$$V_{\text{SME}}^e(R) = \left[\frac{2}{3} \text{tr} \langle p^a p^b \rangle \frac{1}{m_e} \text{tr} \tilde{E}_{ij}^e + \frac{1}{3} \text{tr}_Y \langle p^a p^b \rangle c_{NMN} \frac{1}{m_e} \text{tr}_Y \tilde{E}_{ij}^e \right] , \quad (6.6)$$

¹⁰As a reference, we compare with the corresponding result quoted in [22] (see also [23]),

$$\begin{aligned}
E_{vN} &= 2322.99 (v + \frac{1}{2}) - 67.361 (v + \frac{1}{2})^2 \\
&+ 29.944 N(N + 1) - 1.591 (v + \frac{1}{2})N(N + 1) - 0.0198 (N(N + 1))^2 + \dots
\end{aligned}$$

Comparing with (6.4), we find agreement at better than 1% for B_0 , less than 5% for ω_0 , and within around 10% for the others. This is reasonable given the very simplistic model of the electron wavefunction used in Appendix A, and will be quite sufficient for their rôle below in determining the prefactors of the SME couplings.

¹¹From now on we ignore the distinction between $\hat{\mu}$, \hat{a}_0 , \hat{R}_H and m_e , a_0 , R_H which is of course numerically very small.

where recall the shorthand,

$$c_{NM_N} = \frac{N(N+1) - 3M_N^2}{(2N-1)(2N+3)}, \quad (6.7)$$

and the momentum expectation values and their derivatives take their numerical values as given in Table 1. Substituting these values, we can express the coefficients in (6.5) directly in terms of the SME couplings $\text{tr} \tilde{E}_{ij}^e$ and $\text{tr}_Y \tilde{E}_{ij}^e$ as follows:

$$\begin{aligned} V_{\text{SME}}^e &= \left[0.782 \frac{1}{m_e} \text{tr} \tilde{E}_{ij}^e + 0.120 c_{NM_N} \frac{1}{m_e} \text{tr}_Y \tilde{E}_{ij}^e \right] \\ \delta_{\text{SME}}^e &= \left[-1.000 \frac{1}{m_e} \text{tr} \tilde{E}_{ij}^e - 0.272 c_{NM_N} \frac{1}{m_e} \text{tr}_Y \tilde{E}_{ij}^e \right] \\ B_{\text{SME}}^e &= \lambda \left[-0.666 \frac{1}{m_e} \text{tr} \tilde{E}_{ij}^e - 0.112 c_{NM_N} \frac{1}{m_e} \text{tr}_Y \tilde{E}_{ij}^e \right] \\ \alpha_{\text{SME}}^e &= \lambda^2 \left[-2.152 \frac{1}{m_e} \text{tr} \tilde{E}_{ij}^e - 0.095 c_{NM_N} \frac{1}{m_e} \text{tr}_Y \tilde{E}_{ij}^e \right] \\ D_{\text{SME}}^e &= \lambda^3 \left[-0.979 \frac{1}{m_e} \text{tr} \tilde{E}_{ij}^e - 0.060 c_{NM_N} \frac{1}{m_e} \text{tr}_Y \tilde{E}_{ij}^e \right] \\ x_{\text{SME}}^e &= \lambda \left[-1.629 \frac{1}{m_e} \text{tr} \tilde{E}_{ij}^e - 0.065 c_{NM_N} \frac{1}{m_e} \text{tr}_Y \tilde{E}_{ij}^e \right]. \end{aligned} \quad (6.8)$$

For reference, we also quote here the equivalent results for the coefficients δ_{SME}^n , B_{SME}^n , \dots in the same format. From (5.26), (5.28)-(5.30) and (6.3) we find:

$$\begin{aligned}
\delta_{\text{SME}}^n &= 0.333 \left[\frac{1}{m_p} \text{tr} E_{ij}^p - c_{NMN} \frac{1}{m_p} \text{tr}_Y E_{ij}^p \right] \\
B_{\text{SME}}^n &= 0.333 \lambda \left[\frac{1}{m_p} \text{tr} E_{ij}^p - c_{NMN} \frac{1}{m_p} \text{tr}_Y E_{ij}^p \right] \\
\alpha_{\text{SME}}^n &= 1.133 \lambda^2 \left[\frac{1}{m_p} \text{tr} E_{ij}^p - c_{NMN} \frac{1}{m_p} \text{tr}_Y E_{ij}^p \right] \\
D_{\text{SME}}^n &= 0.667 \lambda^3 \left[\frac{1}{m_p} \text{tr} E_{ij}^p - c_{NMN} \frac{1}{m_p} \text{tr}_Y E_{ij}^p \right] \\
x_{\text{SME}}^n &= 0.820 \lambda \left[\frac{1}{m_p} \text{tr} E_{ij}^p - c_{NMN} \frac{1}{m_p} \text{tr}_Y E_{ij}^p \right]. \tag{6.9}
\end{aligned}$$

We can also write the expressions for the SME corrections to the mean bond length and dissociation energy in this form. From the leading term in (5.20), omitting the weak N -dependence of $O(\lambda^2 N(N+1))$ here, we find

$$\Delta R_{\text{SME}} = \left[1.340 \frac{1}{m_e} \text{tr} \tilde{E}_{ij}^e + 0.226 c_{NMN} \frac{1}{m_e} \text{tr}_Y \tilde{E}_{ij}^e \right]. \tag{6.10}$$

The dissociation energy is defined in (5.21) in terms of $V_{\text{SME}}^e(R_0)$, given in (6.6), $V_{\text{SME}}^e(\infty)$, where $\text{tr} \langle p^a p^b \rangle \rightarrow 1$ and $\text{tr}_Y \langle p^a p^b \rangle \rightarrow 0$, and δ_{SME}^e , which modifies the ground state energy. Substituting from Table 1, we then find

$$\Delta E_{\text{SME}}^{\text{diss}} = \left[-0.105 \frac{1}{m_e} \text{tr} \tilde{E}_{ij}^e - 0.117 c_{NMN} \frac{1}{m_e} \text{tr}_Y \tilde{E}_{ij}^e \right], \tag{6.11}$$

where both ΔR_{SME} and $\Delta E_{\text{SME}}^{\text{diss}}$ in (6.10) and (6.11) are in atomic units.

Finally, to make contact with previous work, we should express $\text{tr} \tilde{E}_{ij}^e$, $\text{tr}_Y \tilde{E}_{ij}^e$ and $\text{tr} E_{ij}^p$, $\text{tr}_Y E_{ij}^p$ directly in terms of the original SME couplings in the Lagrangian (1.1).

It is often convenient in spectroscopy applications to use a spherical harmonic decomposition of the SME couplings. To make the translation, we need to compare the non-relativistic Hamiltonian $H_{\text{SME}}^{\text{NR}}$ in (3.1) with its equivalent in terms of the SME

couplings $c_{n\tilde{j}m}^{\text{NR}}$ and $a_{n\tilde{j}m}^{\text{NR}}$ in the spherical harmonic basis,¹²

$$H_{\text{SME}}^{\text{NR}} = - \sum_{n\tilde{j}m} (c_{n\tilde{j}m}^{\text{NR}} - a_{n\tilde{j}m}^{\text{NR}}) |\mathbf{p}|^n Y_{\tilde{j}m}(\hat{\mathbf{p}}) + \dots \quad (6.12)$$

where \dots represents the spin-dependent couplings in B_k , D_k and F_{ijk} . Specialising to the terms with $n = 2$, we then write

$$p^i p^j = \left(\frac{1}{3} \delta_{ij} + \sum_m C_{ij}^m Y_{2m}(\hat{\mathbf{p}}) \right) |\mathbf{p}|^2, \quad (6.13)$$

and comparing coefficients of the spherical harmonics between (3.1) and (6.12), using (4.19) for C_{ij}^0 , we identify

$$\frac{1}{m} \text{tr} E_{ij} = -3m \frac{1}{\sqrt{4\pi}} (c_{200}^{\text{NR}} - a_{200}^{\text{NR}}), \quad \frac{1}{m} \text{tr}_Y E_{ij} = 3m \sqrt{\frac{5}{4\pi}} (c_{220}^{\text{NR}} - a_{220}^{\text{NR}}). \quad (6.14)$$

with the obvious extension to $\tilde{E}_{ij}^e = E_{ij}^e + \frac{1}{2}(m_e^2/m_p^2)E_{ij}^p$, and E_{ij}^p . In terms of the original SME couplings in (3.2), we therefore have

$$\begin{aligned} \frac{1}{\sqrt{4\pi}} c_{200}^{\text{NR}} &= \frac{1}{3m} (c_{ii} + \frac{3}{2}c_{00}) = \frac{5}{6m} c_{00}, & \frac{1}{\sqrt{4\pi}} a_{200}^{\text{NR}} &= a_{0ii} + a_{000}, \\ \sqrt{\frac{5}{4\pi}} c_{220}^{\text{NR}} &= -\frac{1}{3m} \text{tr}_Y c_{ij}, & \sqrt{\frac{5}{4\pi}} a_{220}^{\text{NR}} &= -\text{tr}_Y a_{0ij}, \end{aligned} \quad (6.15)$$

recalling that $c_{\mu\nu}$ should be chosen to have vanishing spacetime trace [16].

Altogether, equations (5.27) with (6.3), (6.8), (6.9) and (6.14) complete our description of the dependence of the rovibrational energy levels E_{vNMN} of the molecular (anti-)hydrogen ion on the spin-independent SME couplings.

7 Rovibrational transitions

In this final section, we take a first look at how the results in section 6 may be used to constrain the Lorentz and CPT couplings through measurements of the rovibrational transitions H_2^+ , and eventually its antimatter counterpart $\bar{\text{H}}_2^-$, and explain why these

¹²Note the rather unintuitive but now standard notation (see *e.g.* [17]) where mass terms are inserted in these definitions so that both $c_{n\tilde{j}m}^{\text{NR}}$ and $a_{n\tilde{j}m}^{\text{NR}}$ have the *same* dimensions, *i.e.* mass dimension $1 - n$, unlike the corresponding Lagrangian couplings $c_{\mu\nu}$ and $a_{\mu\nu\lambda}$, where $c_{\mu\nu}$ is dimensionless.

offer the possibility of improving existing bounds on the CPT odd spin-independent SME couplings by several orders of magnitude. Further discussion, together with an assessment of current and future experimental possibilities, will be presented elsewhere.

We begin by describing some basic features of the spectrum of the molecular hydrogen ion (see, for example, [12]). Since the $1s\sigma_g$ electron state in H_2^+ is symmetric, the total nucleon state must be antisymmetric under exchange of the two protons – this implies that for *even* N , the two protons are in an antisymmetric spin state $I = 0$ (where \mathbf{I} is the sum of the spins of the two protons), while for *odd* N , the spin state is symmetric so $I = 1$. These two groupings are referred to as Para- and Ortho- H_2^+ respectively. Since H_2^+ is a homonuclear molecule, it has no permanent dipole moment and electric dipole transitions (denoted E1) between rovibrational states (which would allow $\Delta N = 1$ transitions) are forbidden. The remaining possibilities are single-photon electric quadrupole (E2) and two-photon (TP) transitions, for which the selection rule $\Delta N = 0, \pm 2$ applies (with $N = 0 \rightarrow N = 0$ transitions disallowed for E2 but permitted for TP only). These selection rules therefore forbid transitions between the Ortho and Para states, so their spectra are essentially independent of each other.

To illustrate some of the possibilities of constraining the SME couplings by precision measurements of rovibrational transitions, we consider here just the leading coefficients $\delta_{\text{SME}}^{e,p}$ and $B_{\text{SME}}^{e,p}$ from (6.9). In this case,

$$\begin{aligned}
E_{vNMN} = & \left[-\frac{1}{\sqrt{4\pi}} \left(2.35 m_e (\tilde{c}_{200}^{\text{NR}e} - \tilde{a}_{200}^{\text{NR}e}) \right) + \sqrt{\frac{5}{4\pi}} c_{NMN} \left(0.36 m_e (\tilde{c}_{220}^{\text{NR}e} - \tilde{a}_{220}^{\text{NR}e}) \right) \right] \\
& + (v + \frac{1}{2}) \omega_0 \left[1 + \frac{1}{\sqrt{4\pi}} \left(3.00 m_e (\tilde{c}_{200}^{\text{NR}e} - \tilde{a}_{200}^{\text{NR}e}) - m_p (c_{200}^{\text{NR}p} - a_{200}^{\text{NR}p}) \right) \right. \\
& \quad \left. + \sqrt{\frac{5}{4\pi}} c_{NMN} \left(-0.82 m_e (\tilde{c}_{220}^{\text{NR}e} - \tilde{a}_{220}^{\text{NR}e}) - m_p (c_{220}^{\text{NR}p} - a_{220}^{\text{NR}p}) \right) \right] \\
& + \frac{1}{2} \lambda N(N+1) \omega_0 \left[1 + \frac{1}{\sqrt{4\pi}} \left(3.99 m_e (\tilde{c}_{200}^{\text{NR}e} - \tilde{a}_{200}^{\text{NR}e}) - 2 m_p (c_{200}^{\text{NR}p} - a_{200}^{\text{NR}p}) \right) \right. \\
& \quad \left. + \sqrt{\frac{5}{4\pi}} c_{NMN} \left(-0.67 m_e (\tilde{c}_{220}^{\text{NR}e} - \tilde{a}_{220}^{\text{NR}e}) - 2 m_p (c_{220}^{\text{NR}p} - a_{220}^{\text{NR}p}) \right) \right], \tag{7.1}
\end{aligned}$$

with $\tilde{c}_{200}^{\text{NR}e} = c_{200}^{\text{NR}e} + \frac{1}{2} c_{200}^{\text{NR}p}$, *etc.*

The simplest case is a transition where the angular momentum quantum number

is unchanged, *i.e.* $\Delta v \neq 0$ but $\Delta N = 0$ (and $\Delta M_N = 0$). In this case,

$$\begin{aligned} \frac{\Delta E_{\text{SME}}}{\Delta E} &= \delta_{\text{SME}}^e + \delta_{\text{SME}}^p \\ &= \frac{1}{\sqrt{4\pi}} \left[3.00 m_e (\tilde{c}_{200}^{\text{NR}e} - \tilde{a}_{200}^{\text{NR}e}) - 1.00 m_p (c_{200}^{\text{NR}p} - a_{200}^{\text{NR}p}) \right. \\ &\quad \left. + c_{NM_N} \sqrt{5} \left(-0.82 m_e (\tilde{c}_{220}^{\text{NR}e} - \tilde{a}_{220}^{\text{NR}e}) - m_p (c_{220}^{\text{NR}p} - a_{220}^{\text{NR}p}) \right) \right]. \end{aligned} \quad (7.2)$$

This already demonstrates a number of important features. First, even for a purely vibrational transition, the Clebsch-Gordan factor c_{NM_N} arising with the $(n j m) = (220)$ SME couplings implies that the transition frequency is dependent on N and M_N . By comparing transitions with different N , it is then possible to separate the contributions from the (200) and (220) couplings, which can therefore be constrained individually.

Conversely, it is evident from (7.1) that even a purely rotational transition [26] with $\Delta N \neq 0$ but $\Delta v = 0$ will also depend on the vibrational quantum number v through the (220) couplings.

Furthermore, because of the different numerical coefficients of the electron and proton terms in δ_{SME} and B_{SME} , and V_{SME}^e , by comparing different transitions where $\Delta v \neq 0$, $\Delta N = 0$, or $\Delta v = 0$, $\Delta N \neq 0$, or both non-zero, it is also possible to distinguish the contributions from $(\tilde{c}_{200}^{\text{NR}e} - \tilde{a}_{200}^{\text{NR}e})$ and the purely proton coupling $(c_{200}^{\text{NR}p} - a_{200}^{\text{NR}p})$. Similarly for the (220) couplings. A relatively small number of rovibrational transitions in H_2^+ could therefore lead to precision constraints on all four types of $(c_{n j m}^{\text{NR}} - a_{n j m}^{\text{NR}})$ couplings in (7.1).

Finally, if similar precision experiments become possible with the antihydrogen molecular ion [27–30], then because the $c_{n j m}^{\text{NR}}$ couplings are CPT even while the $a_{n j m}^{\text{NR}}$ couplings are CPT-odd, taking the difference of the H_2^+ and $\bar{\text{H}}_2^-$ spectra would isolate the dependence on the $a_{n j m}^{\text{NR}}$ couplings. This would allow individual constraints to be placed on all 8 SME couplings in (7.1).

To see why these constraints are potentially so powerful for the molecular ions, we should compare with the equivalent transitions with atomic hydrogen and antihydrogen. Keeping only the spin-independent SME couplings, we find for the $1S_d - 2S_d$ transition [5, 19] measured for antihydrogen by ALPHA [7] (where the suffix d labels the particular hyperfine state),

$$\frac{\Delta E_{1S_d - 2S_d}^{\text{SME}}}{\Delta E_{1S - 2S}} = \frac{2m_e}{\sqrt{4\pi}} \left[(c_{200}^{\text{NR}e} - a_{200}^{\text{NR}e}) + (c_{200}^{\text{NR}p} - a_{200}^{\text{NR}p}) \right]. \quad (7.3)$$

Notice this is only sensitive to the $(n j m) = (200)$ couplings.

To access a transition sensitive to the $(n j m) = (220)$ couplings in (anti-)hydrogen, we need to consider a state with electron orbital momentum $\ell \neq 0$ (in the same way that we require $N \neq 0$ to access the (220) contributions to the rovibrational states in (7.1)). ALPHA has measured the $1S_d-2P_{c-}$ transition [9] for which we can show [5, 19],

$$\frac{\Delta E_{1S_d-2P_{c-}}^{\text{SME}}}{\Delta E_{1S-2S}} = \frac{2m_e}{\sqrt{4\pi}} \left[(c_{200}^{\text{NR}e} - a_{200}^{\text{NR}e}) + (c_{200}^{\text{NR}p} - a_{200}^{\text{NR}p}) - \frac{\sqrt{5}}{30} (1 + 3 \cos 2\eta) \left((c_{220}^{\text{NR}e} - a_{220}^{\text{NR}e}) + (c_{220}^{\text{NR}p} - a_{220}^{\text{NR}p}) \right) \right], \quad (7.4)$$

where $\cos \eta$ is a magnetic field dependent mixing angle.

This brings us to the key point. Focusing on the CPT violating couplings, the two-photon $1S-2S$ transition in (anti-)hydrogen constrains the combination

$$m_e (a_{200}^{\text{NR}e} + a_{200}^{\text{NR}p}) \lesssim R_{1S-2S}, \quad (7.5)$$

where R_{1S-2S} is the relative precision of the measurement. ALPHA has measured this transition for antihydrogen with a precision $R_{1S-2S} \simeq 2 \times 10^{-12}$ [7], while a precision of $O(10^{-15})$ is known for hydrogen [31, 32]. Knowing this, the single-photon $1S-2P$ transition, which is measured by ALPHA with the much weaker precision $R_{1S-2P} \simeq 10^{-8}$ [9], constrains the (220) combination,

$$m_e (a_{220}^{\text{NR}e} + a_{220}^{\text{NR}p}) \lesssim R_{1S-2P}. \quad (7.6)$$

With just four measurements, $1S-2S$ and $1S-2P$ for hydrogen and antihydrogen, we are able to constrain only the combinations (7.5), (7.6) of electron and proton couplings, and similar for the $c_{n j m}^{\text{NR}}$. Crucially, *both* the electron and proton couplings are multiplied by m_e .

In contrast, for H_2^+ , by measuring only a small number of rovibrational transitions as indicated above, together with the equivalent for $\overline{\text{H}}_2^-$, we have sufficient data to constrain all 8 coefficients. Denoting the precisions generically by R_{rovib} , in this case we find the constraints,

$$m_e (a_{200}^{\text{NR}e} + \frac{1}{2} a_{200}^{\text{NR}p}) \lesssim R_{rovib}, \quad m_p a_{200}^{\text{NR}p} \lesssim R_{rovib}, \quad (7.7)$$

and

$$m_e (a_{220}^{\text{NR}e} + \frac{1}{2} a_{220}^{\text{NR}p}) \lesssim R_{rovib}, \quad m_p a_{220}^{\text{NR}p} \lesssim R_{rovib}, \quad (7.8)$$

with equivalent bounds for the c_{njm}^{NR} . Here, we have written out in full the couplings $\tilde{c}_{njm}^{\text{NR}e}$ and $\tilde{a}_{njm}^{\text{NR}e}$. Notice that the bounds on the proton SME couplings arising from their indirect influence on the electron Schrödinger equation have the same m_e mass dependence as those found in the atomic transitions. This is not true of the proton couplings arising directly in the nucleon Schrödinger equation, which involve m_p itself.

So not only do the rovibrational transitions allow us to constrain the electron and proton couplings separately, the constraint on the proton couplings $a_{200}^{\text{NR}p}$ and $a_{220}^{\text{NR}p}$ is *enhanced* by a factor $m_p/m_e \sim 10^3$ compared to the atomic transitions. This is in addition to the potential enhancement from the greater precision of frequency measurements for the rovibrational transitions, which of course is especially marked for the (220) couplings where the precision of the $1S$ - $2P$ measurement in antihydrogen is necessarily 4 orders of magnitude below that achieved for $1S$ - $2S$.

In practice, by far the most stringent bounds on the proton ($c_{2jm}^{\text{NR}p} - a_{2jm}^{\text{NR}p}$) couplings arise not from atomic hydrogen transitions but from those associated with heavier elements, in particular ^{133}Cs clock transitions [33–35]. However, unlike the molecular ions discussed here, these do not have accessible antimatter counterparts and cannot isolate the CPT odd couplings. From the standpoint of the SME, therefore, the unique strength of spectroscopy of the (anti-)molecular ions H_2^+ and $\overline{\text{H}}_2^-$ is in providing a direct test of CPT symmetry at high precision.

So far, we have only considered the rovibrational states to be described by quantum numbers v, N, M_N and have neglected spin (see [36–38]). In general, the $1s\sigma_g$ states in H_2^+ will be labelled as $|v N I S F J M_J\rangle$, according to the angular momentum addition scheme $\mathbf{F} = \mathbf{I} + \mathbf{S}$, where \mathbf{I} and \mathbf{S} are the total nucleon and electron spins respectively, followed by $\mathbf{J} = \mathbf{N} + \mathbf{F}$.

The hyperfine structure is then determined by a Hamiltonian incorporating 5 combinations of spin-spin and spin-orbit interactions, with known coefficients calculated at $O(\alpha^2)$ to six-figure precision in QED [36]. This simplifies greatly for the case of Para- H_2^+ and we illustrate our results for this case here. The energy eigenstates, at zero background magnetic field, are then $|v N S J M_J\rangle$ with $S = 1/2$ always and $\mathbf{J} = \mathbf{N} + \mathbf{S}$. The corresponding hyperfine interaction is simply,

$$H_{\text{HFS}} = c_e(v, N) \mathbf{N} \cdot \mathbf{S} = \frac{1}{2} c_e(v, N) (\mathbf{J}^2 - \mathbf{N}^2 - \mathbf{S}^2). \quad (7.9)$$

The values of $c_e(v, N)$ for low values of v and N are given in Table 1 of [36]. It follows

directly that the rovibrational energies are split by the value of $J = N \pm 1/2$ as follows,

$$\begin{aligned}\Delta E_{\text{HFS}} &= \frac{1}{2} c_e(v, N) N, \quad (J = N + \frac{1}{2}) \\ &= -\frac{1}{2} c_e(v, N) (N + 1), \quad (J = N - \frac{1}{2}),\end{aligned}\quad (7.10)$$

and are degenerate with respect to M_J .

To calculate the SME contributions to the hyperfine states, we first express the eigenstates $|J M_J\rangle$ in terms of the $|M_N M_S\rangle$ basis states through Clebsch-Gordan coefficients as follows,

$$|J M_J\rangle = \sum_{M_S} C_{N M_N, \frac{1}{2} M_S}^{J M_J} |M_N M_S\rangle, \quad (M_N = M_J - M_S). \quad (7.11)$$

Now, at the point (4.16) for the electron $V_{\text{SME}}^e(R)$, or (5.24) for the proton \tilde{V}_{SME}^n , our derivation of the rovibrational energies requires the evaluation of $\sum_M C_{ij}^M Y_{2M}$ between eigenstates, taken there to be $|v N M_N\rangle$. Using the hyperfine states $|J M_J\rangle$ instead, we find

$$\begin{aligned}E_{ij} \sum_M C_{ij}^M \langle J M_J | Y_{2M} | J M_J \rangle \\ &= E_{ij} \sum_{M_S} C_{ij}^0 \left(C_{N M_N, \frac{1}{2} M_S}^{J M_J} \right)^2 \langle M_N M_S | Y_{20} | M_N M_S \rangle \\ &= -\frac{1}{3} \text{tr}_Y E_{ij} \sum_{M_S} \left(C_{N M_N, \frac{1}{2} M_S}^{J M_J} \right)^2 c_{N(M_J - M_S)},\end{aligned}\quad (7.12)$$

in terms of the factor $c_{N M_N}$ in (6.7). The results of these calculations are presented in Paper 2 [20], showing in detail how the spin-independent SME couplings break the degeneracy with respect to M_J of the hyperfine energy levels.

In practice, spectroscopy will be performed in a background magnetic field, which we may use to define the 3-axis of the EXP frame, $\mathbf{B} = (0, 0, B)$. The rovibrational energies will therefore acquire a shift due to the Zeeman effect. Restricting again to Para- H_2^+ , the Zeeman Hamiltonian is

$$H_Z = g_e \mu_B \mathbf{S} \cdot \mathbf{B} - g_m(v, N) \mu_B \mathbf{N} \cdot \mathbf{B}, \quad (7.13)$$

where the effective g -factor $g_m(v, N)$ depends on the rovibrational quantum numbers [20, 37]. It is $O(m_e/m_p)$ so the electron spin dominates the energy shifts. For large B , where the hyperfine splitting is negligible compared to the Zeeman effect, the combined

hyperfine-Zeeman eigenstates become approximately just the $|v N S M_N M_S\rangle$ states. For intermediate magnetic fields, apart from the extremal states $|J = N + \frac{1}{2}, M_J = \pm(N + \frac{1}{2})\rangle \equiv |M_N = \pm N, M_S = \pm \frac{1}{2}\rangle$ where the two bases coincide, the remaining $4N$ hyperfine-Zeeman eigenstates are mixed pairwise, with $2N$ B -dependent mixing angles.¹³

Our original derivation of the rovibrational energy levels therefore applies directly in the large B regime where the eigenstates are essentially given by $|M_N M_S\rangle$, and the results above with c_{NM_N} hold, showing the extra M_N dependence of the energy levels due to the SME couplings. For intermediate values of the magnetic field, the corresponding SME energies involving c_{220}^{NR} and a_{220}^{NR} will depend in an individual way on the state mixing, described in detail in Paper 2.

Our focus in this paper has been on the spin-independent SME couplings, for reasons given above. Inclusion of the spin-dependent couplings is in principle a straightforward extension of the results given here, though inevitably more complicated in general given the spin dependence of the hyperfine states. Again, our results are fully described in Paper 2.

Finally, apart from precision measurements of rovibrational energy levels, including a comparison of H_2^+ and $\overline{\text{H}}_2^-$ as a direct CPT test, Lorentz symmetry breaking would reveal itself through annual (and sidereal) variations in the transition frequencies resulting from the SME coupling contributions derived above. This analysis is well-known (see *e.g.* [18]) and we only comment briefly here.

The first step is to rewrite the SME couplings in components referred to the standard SUN frame (see section 3). In general this involves a rotation from the EXP to SUN frames, which depends on the location and orientation of the background magnetic field of the particular experiment. Note, however, that this rotation does not affect the isotropic (200) couplings, which retain their form in the SUN frame.

These SUN frame couplings are then subject to a Lorentz transformation with velocity v_{\oplus} of $O(10^{-4})$ corresponding to the Earth's rotation around the Sun, resulting in small periodic variations with the Earth's orbit. In SUN frame coordinates (T, X, Y, Z) ,

¹³For an explicit example, the hyperfine-Zeeman states in Para- H_2^+ with $N = 2$ and the associated energy curves as a function of B interpolating between pure hyperfine and large- B Zeeman states, see sections C, D and Fig. 2 of the Supplementary Material of [12] and Paper 2 [20].

the orbital velocity is

$$\mathbf{v}_\oplus = v_\oplus \left(\sin \Omega_\oplus T \mathbf{e}_X - \cos \Omega_\oplus T (\cos \eta \mathbf{e}_Y + \sin \eta \mathbf{e}_Z) \right), \quad (7.14)$$

where Ω_\oplus is the orbital frequency and $\eta = 23.4^\circ$ is the tilt angle between the Earth's equator and the orbital plane. The isotropic SME couplings in the rovibrational energy levels are simply $\frac{1}{\sqrt{4\pi}} c_{200}^{\text{NR}} = \frac{1}{3m} \left(\frac{3}{2} c_{TT} + c_{KK} \right) = \frac{5}{6m} c_{TT}$ and $\frac{1}{\sqrt{4\pi}} a_{200}^{\text{NR}} = a_{TTT} + a_{TKK}$. Applying a Lorentz transformation with \mathbf{v}_\oplus then gives the periodic variation of the combinations of isotropic SME couplings appearing in the rovibrational energies (7.1) as,

$$\begin{aligned} \frac{1}{\sqrt{4\pi}} \delta_\oplus (c_{200}^{\text{NR}} - a_{200}^{\text{NR}}) &= v_\oplus \sin \Omega_\oplus T \left(\frac{5}{3m} c_{XT} - 5a_{XTT} - a_{XKK} \right) \\ &\quad - v_\oplus \cos \Omega_\oplus T \left(\cos \eta \left(\frac{5}{3m} c_{YT} - 5a_{YTT} - a_{YKK} \right) \right. \\ &\quad \left. + \sin \eta \left(\frac{5}{3m} c_{ZT} - 5a_{ZTT} - a_{ZKK} \right) \right). \quad (7.15) \end{aligned}$$

Similar results for the non-isotropic combination $(c_{220}^{\text{NR}} - a_{220}^{\text{NR}})$ depend in detail on the orientation of the EXP frame for a specific experiment. Note that the variations introduce a dependence on different components of the SME couplings from those appearing in the rovibrational energies themselves. Detection of such annual variations of the ultra-precise rovibrational transition frequencies would be a clear signal of Lorentz, and potentially CPT, violation.

Acknowledgements

I am grateful to Stefan Eriksson for motivating this research and for many helpful discussions during its progress. I would also like to thank the Higgs Centre for Theoretical Physics at the University of Edinburgh for hospitality in the course of this work and the CERN Theory Division for Visiting Scientist support.

A Solution of the electron Schrödinger equation

In this appendix, we give some details of the solution of the electron Schrödinger equation in the absence of Lorentz and CPT violation. In particular, we determine the energy eigenvalue $E_e(R)$, which carries through to the nucleon Schrödinger equation in the Born-Oppenheimer analysis as the inter-nucleon potential $V_M(R)$. We also calculate the R -dependence of the momentum expectation values $\langle p^a p^b \rangle$, which are needed as input in determining the potential $V_{\text{SME}}^e(R)$ in (3.6).

From the main text, the Schrödinger equation for the electron wavefunction $\psi(\mathbf{r}; R)$ is

$$\left(-\frac{1}{2\hat{\mu}} \nabla_{\mathbf{r}}^2 + V_{mol}(R, r_{1e}, r_{2e}) \right) \psi(\mathbf{r}; R) = E_e(R) \psi(\mathbf{r}; R) , \quad (\text{A.1})$$

with the binding potential $V_{mol}(R, r_{1e}, r_{2e})$ given in (2.2). The basic idea of the solution is to make an *ansatz* for the electron wavefunction in the $1s\sigma_g$ state comprising a sum of hydrogen-like $1s$ wave functions, *viz.*

$$\psi(\mathbf{r}; R) = \frac{1}{\sqrt{2(1 + I_0(R))}} (\psi_H(r_{1e}; R) + \psi_H(r_{2e}; R)) , \quad (\text{A.2})$$

where

$$\psi_H(r; R) = \sqrt{\frac{\gamma(R)^3}{\pi \hat{a}_0^3}} e^{-\gamma(R)r/\hat{a}_0} . \quad (\text{A.3})$$

and the “overlap function” $I_0(R)$ is required to normalise the wavefunction. Explicitly,

$$I_0(R) = \int d^3\mathbf{r} \psi_H(r_{1e}) \psi_H(r_{2e}) . \quad (\text{A.4})$$

The necessity of including the scaling factor $\gamma(R)$ of the effective Bohr radius in (A.3) is seen by considering the limits of large and small nucleon separation. As $R \rightarrow \infty$, one of r_{1e} or r_{2e} in (A.3) becomes large and so the total wavefunction reduces to a single $1s$ hydrogen state. The molecule has dissociated leaving a hydrogen atom and an isolated proton. In this limit, therefore, we require $\gamma(R) \rightarrow 1$, recovering the original Bohr radius. At the other extreme, as $R \rightarrow 0$ the two nucleons coalesce and the wavefunction should reduce to that of a hydrogen-like atom with $Z = 2$. In this case the dependence on the Bohr radius implies $\gamma(R) \rightarrow 2$. We see below how this is realised in the explicit numerical solutions for the energies and momenta.

In (A.3), we have introduced the notation $\hat{a}_0 = 1/\alpha\hat{\mu}$ for the “reduced Bohr radius” appropriate to the reduced electron mass $\hat{\mu}$ in section 2. Together with the corresponding “reduced Rydberg constant” $\hat{R}_H = \frac{1}{2}\alpha^2\hat{\mu} = 1/(2\hat{a}_0^2\hat{\mu})$, this defines the units of

length and energy used from now on. Rescaling to these “atomic units”, the electron Schrödinger equation is simply

$$\left(-\nabla_{\mathbf{r}}^2 + 2\left(\frac{1}{R} - \frac{1}{r_{1e}} - \frac{1}{r_{2e}}\right)\right)\psi(\mathbf{r}; R) = E_e(R)\psi(\mathbf{r}; R), \quad (\text{A.5})$$

where all quantities are now dimensionless.

To calculate the energy eigenvalues $E_e(R)$, we need a number of elementary integrals, all of which can be evaluated analytically for $\gamma(R) = 1$ [21]. Defining the kinetic and potential energies as $K(R)$ and $U(R)$ respectively, we have

$$K(R) = -\langle\psi|\nabla_{\mathbf{r}}^2|\psi\rangle, \quad U(R) = 2\langle\psi|\frac{1}{R} - \frac{1}{r_{1e}} - \frac{1}{r_{2e}}|\psi\rangle. \quad (\text{A.6})$$

First, for the overlap function we need

$$I_0 = \frac{1}{\pi} \int d^3\mathbf{r} e^{-r_{1e}} e^{-r_{2e}} = \left(1 + R + \frac{1}{3}R^2\right)e^{-R}. \quad (\text{A.7})$$

Then, for the potential energy,

$$I_1 = \frac{1}{\pi} \int d^3\mathbf{r} \frac{1}{r_{1e}} e^{-r_{1e}} e^{-r_{1e}} = 1, \quad (\text{A.8})$$

$$I_2 = \frac{1}{\pi} \int d^3\mathbf{r} \frac{1}{r_{1e}} e^{-r_{2e}} e^{-r_{2e}} = \frac{1}{R} - \frac{1}{R}(1+R)e^{-2R}, \quad (\text{A.9})$$

$$I_3 = \frac{1}{\pi} \int d^3\mathbf{r} \frac{1}{r_{1e}} e^{-r_{1e}} e^{-r_{2e}} = (1+R)e^{-R}, \quad (\text{A.10})$$

so that in total, with $\gamma(R)$ set to 1,

$$U_1(R) = \frac{2}{R} - \frac{2}{(1+I_0)}(I_1 + I_2 + 2I_3). \quad (\text{A.11})$$

Here, and below, we use the suffix 1 to indicate that the associated quantity is evaluated with $\gamma(R) \rightarrow 1$. For the kinetic energy, a similar calculation gives

$$K_1(R) = -1 + \frac{2}{(1+I_0)}(I_1 + I_3). \quad (\text{A.12})$$

Separating out the hydrogen 1s energy in reduced Rydberg units, $\hat{E}_{1s} = -1$, we may write the total energy eigenvalue as

$$\begin{aligned} E_{e1}(R) &= K_1(R) + U_1(R) \\ &= \hat{E}_{1s} + \frac{2}{R} - \frac{2}{(1+I_0)}(I_2 + I_3). \end{aligned} \quad (\text{A.13})$$

This shows the typical Morse function form, with a minimum at $R_0 = 2.493$.

To find the Lorentz and CPT violating contributions $V_{\text{SME}}^e(\mathbf{R})$, we also need the expectation values of the components of the momenta, specifically

$$\langle p^a p^b \rangle = - \int d^3 \mathbf{r} \psi(\mathbf{r}; R) \frac{\partial}{\partial x_a} \frac{\partial}{\partial x_b} \psi(\mathbf{r}; R) . \quad (\text{A.14})$$

The required integrals in this case include

$$J_1 = -\frac{1}{\pi} \int d^3 \mathbf{r} e^{-r_{1e}} \frac{\partial^2}{\partial x^2} e^{-r_{1e}} = \frac{1}{3} , \quad (\text{A.15})$$

$$J_2 = -\frac{1}{\pi} \int d^3 \mathbf{r} e^{-r_{2e}} \frac{\partial^2}{\partial x^2} e^{-r_{2e}} = \frac{1}{3} , \quad (\text{A.16})$$

$$J_3 = -\frac{1}{\pi} \int d^3 \mathbf{r} e^{-r_{1e}} \frac{\partial^2}{\partial x^2} e^{-r_{2e}} = \frac{1}{3}(1+R)e^{-R} . \quad (\text{A.17})$$

Cylindrical symmetry in the MOL frame ensures identical results with derivatives $\partial^2/\partial y^2$, while for $\partial^2/\partial z^2$ we find $J_3 \rightarrow \frac{1}{3}(1+R-R^2)e^{-R}$ with J_1 and J_2 unchanged. It is also apparent from the evaluation that the mixed terms, $\langle p^a p^b \rangle$ with $a \neq b$, vanish.

Collecting these results we find, again with $\gamma(R)$ set to 1,

$$\langle p^x p^x \rangle_1 = \langle p^y p^y \rangle_1 = \frac{1}{3} \frac{1}{(1+I_0)} (1 + (1+R)e^{-R}) , \quad (\text{A.18})$$

and

$$\langle p^z p^z \rangle_1 = \frac{1}{3} \frac{1}{(1+I_0)} (1 + (1+R-R^2)e^{-R}) , \quad (\text{A.19})$$

and as an immediate consistency check we verify $K_1 = \langle p^x p^x \rangle_1 + \langle p^y p^y \rangle_1 + \langle p^z p^z \rangle_1$.

Now introduce the rescaling factor $\gamma(R)$ into the electron wavefunctions. By inspection, we see that the kinetic and potential energies and the momentum expectation values now become

$$K(R) = \gamma(R)^2 K_1(\gamma(R)R) , \quad U(R) = \gamma(R) U_1(\gamma(R)R) , \quad (\text{A.20})$$

and

$$\langle p^a p^b \rangle(R) = \gamma(R)^2 \langle p^a p^b \rangle_1(\gamma(R)R) . \quad (\text{A.21})$$

The aim here is to find a function $\gamma(R)$ which minimises the energy $E_e(R)$, where

$$E_e(R) = \gamma(R)^2 K_1(\gamma(R)R) + \gamma(R) U_1(\gamma(R)R) . \quad (\text{A.22})$$

We use a numerical method¹⁴, the idea being to choose a discrete set of values $R = R_n$ and for each n find the value of $\gamma(R_n)$ for which the energy $E_e(R_n)$ is minimised. We then construct an interpolating function $\gamma(R)$ to fit this set of values. The result is the function $\gamma(R)$ shown in Fig. 3. Notice that this does indeed satisfy the requirement that $\gamma(0) = 2$ and $\gamma(R) \rightarrow 1$ for large R , though this is not imposed as a constraint.

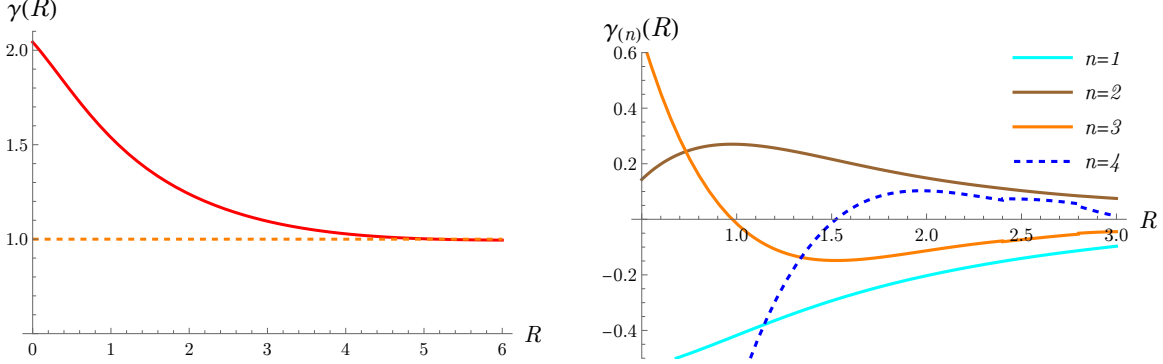


Figure 3. The interpolating function $\gamma(R)$ giving the appropriate scaling of the electron wave function as the inter-nucleon distance R is varied. The right hand figure shows its first four derivatives in the vicinity of the minimum of the potential at $R_0 = 2.003$. See Table 1.

Given $\gamma(R)$, the energy and momentum expectation values are found from (A.22) and (A.21). These are shown in Figs. 4 and 5. A few comments are worth making here. Note that the energy $E_e(R)$ has a deeper minimum with the improved ansatz with the interpolating function $\gamma(R)$, and it occurs at the smaller value $R_0 = 2.003$. This gives a much improved agreement with the measured dissociation energy for H_2^+ , though still not sufficiently deep. However, the value for the fundamental vibration frequency $\omega_0 = \sqrt{V_M''(R_0)/\mu} = 0.020 R_H$, in good agreement with the measured value.

As expected, for large R where the molecule has effectively separated, $E_e(R)$ tends to the atomic $1s$ level $\hat{E}_{1s} = -1$. Moreover, we numerically confirm the analytic results $K(R) \rightarrow 1$ and $U(R) \rightarrow -2$ as $R \rightarrow \infty$, in agreement with the virial theorem for a Coulomb interaction.¹⁵ On the other hand, for $R \rightarrow 0$, if we set aside the divergent

¹⁴What follows is our interpretation of the method applied in [11], and we may compare our numerical results with the table of values for $E_e(R_0)$, $\gamma(R_0)$, $\langle p^a p^b \rangle(R_0)$ and their derivatives at R_0 quoted there.

¹⁵The virial theorem for a power-law potential $V(x)$ states

$$2\langle K \rangle = \left\langle x \frac{dV}{dx} \right\rangle,$$

so for the Coulomb potential in A.5, and neglecting the inter-nucleon repulsion which tends to zero

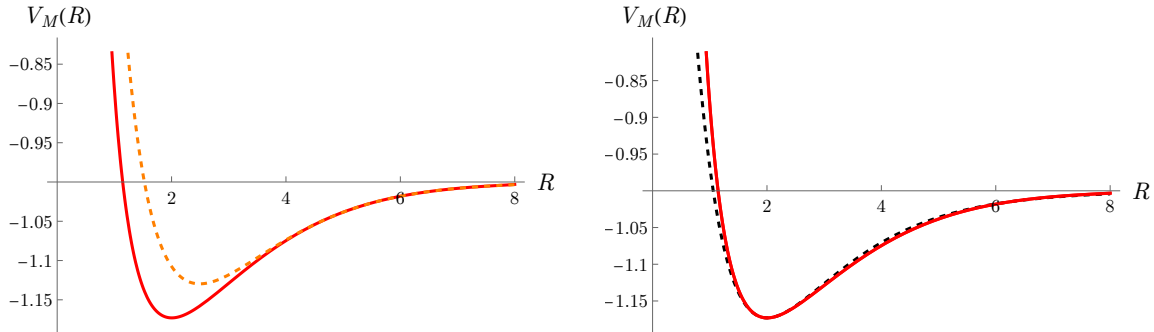


Figure 4. The nucleon potential $V_M(R) \equiv E_e(R)$ as the inter-nucleon distance, or bond length, R is varied. The minimum is at $R_0 = 2.003$. The left hand figure shows a comparison with the equivalent with the scaling factor $\gamma(R)$ left fixed equal to 1 (orange, dashed). The right hand figure shows the comparison with a Morse potential (black, dashed) with its two free parameters set to match the potential minimum $V_M(R_0)$ and curvature $V_M''(R_0)$.

nucleon-nucleon interaction term $2/R$ in the potential, we find with $\gamma(0) = 2$ that $K(0) \rightarrow 4$ and $U(0) \rightarrow -8$, again satisfying the virial theorem and confirmed numerically in Fig. 4. A comparison of $V_M(R)$ with the phenomenological Morse potential¹⁶ is also shown in Fig. 4.

We can also check the asymptotic behaviour of the momentum expectation values analytically. For both large and small R , where the molecule becomes effectively an atom, spherical symmetry is restored so all the expectation values in (A.18) and (A.19) are equal, with $\langle p^a p^a \rangle = \langle p^2 \rangle / 3 = K/3$. This is confirmed numerically in Fig. 5 where for large R , this implies $2\langle K \rangle = -\langle U \rangle$.

¹⁶The Morse potential is a two-parameter function,

$$V_{Morse}(R) = D_e(1 - e^{-ax})^2 - D_e$$

where $x = R - R_0$. To make the comparison, we fit the parameters D_e and a to the value of $V_M(R)$ and its second derivative at R_0 , *viz.* $D_e = -V_M(R_0)$ and $a^2 = -\frac{1}{2}V_M''(R_0)/(1+V_M(R_0))$, so $D_e = 0.173$ and $a = 0.735$ in atomic units. The vibrational energy levels in the Morse potential are exact, truncating at $O(v + \frac{1}{2})^2$,

$$E_v = (v + \frac{1}{2})\omega_0 - \frac{\omega_0}{4D_e}(v + \frac{1}{2})^2\omega_0,$$

where the fundamental frequency is $\omega_0 = a\sqrt{2D_e/\mu} = 0.020$. The sign of the coefficient $\omega_0/4D_e = 0.029$ ensures that the spacing between vibrational energy levels reduces as v increases, unlike a SHO. This parameter is equivalent to the $x_0 = 0.033$ of (6.3) calculated from purely anharmonic terms in the full numerical potential $V_M(R)$. This shows excellent agreement and gives further confidence that our analysis is providing a good characterisation of the rovibrational spectrum at the required precision for computing SME corrections.

we observe all the $\langle p^a p^a \rangle$ becoming equal and tending to $1/3$ for $R \rightarrow \infty$ and $4/3$ for $R \rightarrow 0$.

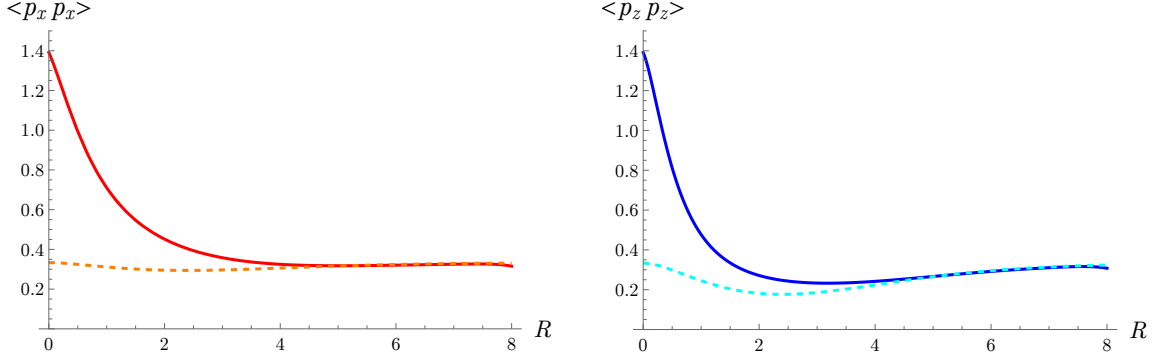


Figure 5. The momentum expectation values from (A.18), (A.19) and (A.21) as a function of the bond length R . The left hand figure shows $\langle p^x p^x \rangle$ evaluated with $\gamma(R)$ and (dashed curve) fixed equal to 1. The right hand figure is the same for $\langle p^z p^z \rangle$.

Derivative	0	1	2	3	4
V_M	-1.173	0	0.187	-0.492	1.237
$\langle p^x p^x \rangle$	0.451	-0.146	0.146	-0.162	0.229
$\langle p^z p^z \rangle$	0.271	-0.083	0.133	-0.188	0.349
γ	1.238	-0.203	0.148	-0.113	0.102
$\text{tr} \langle p^a p^b \rangle$	1.173	-0.375	0.424	-0.512	0.808
$\text{tr}_Y \langle p^a p^b \rangle$	0.360	-0.126	0.026	0.052	-0.239

Table 1. The values and first few derivatives of the inter-nucleon potential $V_M(R)$, the momentum expectation values $\langle p^x p^x \rangle$ and $\langle p^z p^z \rangle$, and the interpolating function $\gamma(R)$ used in their construction, all evaluated at the minimum $R_0 = 2.003$ of $V_M(R)$. All numbers are expressed in atomic units, with energies in terms of the reduced Rydberg constant \hat{R}_H and lengths in terms of the reduced Bohr radius \hat{a}_0 .

Finally, for the analysis of the rovibrational levels in sections 5 and 6, we need

explicit values for the first few derivatives of the energy and momentum expectation values at the minimum R_0 of the improved potential $V_M(R) = E_e(R)$. These are evaluated numerically from the functions plotted above, and the required values are shown in Table 1, which may be compared with [11]. Recall that cylindrical symmetry ensures that $\langle p^x p^x \rangle = \langle p^y p^y \rangle$. We also include here the combinations $\text{tr} \langle p^a p^b \rangle = \langle p^x p^x \rangle + \langle p^y p^y \rangle + \langle p^z p^z \rangle$ and $\text{tr}_Y \langle p^a p^b \rangle = \langle p^x p^x \rangle + \langle p^y p^y \rangle - 2\langle p^z p^z \rangle$ which appear as coefficients in the SME potential V_{SME}^e .

B Rovibrational energy levels - perturbation method

In this appendix, we present a systematic perturbative method to evaluate the rovibrational energy levels incorporating the Lorentz and CPT violating corrections. This provides an important consistency check on the results obtained in section 4.

The idea is to expand all the contributions to the potential in the nucleon Schrödinger equation (3.6) about the minimum R_0 of the inter-nucleon potential $V_M(R)$, then evaluate the energy corrections as perturbations about the leading SHO approximation. As we see, this turns out to give a systematic perturbative expansion in the small parameter $\lambda = 1/\mu\omega_0 R_0^2$ identified previously. We therefore write,

$$\begin{aligned} V_M(R) + V_N(R) + V_{\text{SME}}^e(R) \\ = V_M(R_0) + V_N(R_0) + V_{\text{SME}}^e(R_0) + \frac{1}{2}\mu\omega_0^2 x^2 + \delta V_M(x) + \delta V_N(x) + \delta V_{\text{SME}}^e(x) , \end{aligned} \quad (\text{B.1})$$

where here $x = R - R_0$ and $V_N(R) = N(N+1)/2\mu R^2$, so $V_N(R_0) = \frac{1}{2}\lambda\omega_0 N(N+1)$. Then,

$$\begin{aligned} \delta V_M &= \frac{1}{6}V_M''' x^3 + \frac{1}{24}V_M^{(4)} x^4 + \dots \\ \delta V_N &= \lambda\omega_0 N(N+1) \left(-\frac{x}{R_0} + \frac{3}{2}\left(\frac{x}{R_0}\right)^2 - 2\left(\frac{x}{R_0}\right)^3 + \dots \right) \\ \delta V_{\text{SME}}^e &= V_{\text{SME}}^{e'} x + \frac{1}{2}V_{\text{SME}}^{e''} x^2 + \frac{1}{6}V_{\text{SME}}^{e'''} x^3 + \dots \end{aligned} \quad (\text{B.2})$$

We start from the SHO with potential $\frac{1}{2}V_M'' x^2 = \frac{1}{2}\mu\omega_0^2 x^2$ and construct the usual states labelled by integers $|v\rangle$ with energy eigenvalues $E_v^{(0)} = (v + \frac{1}{2})\omega_0$. We will need the expressions for the energy levels up to 3rd order in perturbation theory, *viz.*

$$E_v = E_v^{(0)} + E_v^{(1)} + E_v^{(2)} + E_v^{(3)} , \quad (\text{B.3})$$

with, for a perturbation δV in the potential,

$$\begin{aligned}
E_v^{(1)} &= \langle v | \delta V | v \rangle , \\
E_v^{(2)} &= \sum_{k \neq v} \frac{1}{(E_v^{(0)} - E_k^{(0)})} \langle v | \delta V | k \rangle \langle k | \delta V | v \rangle , \\
E_v^{(3)} &= \sum_{k \neq v} \sum_{\ell \neq v} \frac{1}{(E_v^{(0)} - E_k^{(0)})(E_v^{(0)} - E_\ell^{(0)})} \langle v | \delta V | k \rangle \langle k | \delta V | \ell \rangle \langle \ell | \delta V | v \rangle \\
&\quad - \sum_{k \neq v} \frac{1}{(E_v^{(0)} - E_k^{(0)})^2} |\langle v | \delta V | k \rangle|^2 \langle v | \delta V | v \rangle . \tag{B.4}
\end{aligned}$$

The states here are all understood to be the unperturbed SHO states; clearly the notation with states carrying a label $|v\rangle^{(0)}$ throughout is too cumbersome. The perturbation δV in our case is the sum of the anharmonic potential, angular momentum and SME terms in (2.2), $\delta V = \delta V_M + \delta V_N + \delta V_{\text{SME}}^e$.

Now at first order, only even powers of x contribute to the expectation values, so we have,

$$E_v^{(1)} = \left(\frac{3}{2} \lambda \omega_0 N(N+1)/R_0^2 + \frac{1}{2} V_{\text{SME}}^{e''} \right) \langle v | x^2 | v \rangle + \frac{1}{24} (V_M^{(4)} + V_{\text{SME}}^{e(4)}) \langle v | x^4 | v \rangle . \tag{B.5}$$

The expectation values here and throughout this section are evaluated using elementary methods, expanding the powers of x in terms of raising and lowering operators using,

$$\frac{1}{R_0} x = \sqrt{\frac{\lambda}{2}} (a + a^\dagger) \quad \text{with} \quad a^\dagger |v\rangle = \sqrt{v+1} |v+1\rangle , \quad a |v\rangle = \sqrt{v} |v-1\rangle . \tag{B.6}$$

Then, evaluating

$$\frac{1}{R_0^2} \langle v | x^2 | v \rangle = (v + \frac{1}{2}) \lambda , \quad \text{and} \quad \frac{1}{R_0^4} \langle v | x^4 | v \rangle = \frac{3}{2} \left((v + \frac{1}{2})^2 + \frac{1}{4} \right) \lambda^2 , \tag{B.7}$$

and dropping the constant term, which adds negligibly to $V_M(R_0)$, $V_{\text{SME}}^e(R_0)$ and the dissociation energy, we find

$$\begin{aligned}
E_v^{(1)} &= \frac{3}{2} (v + \frac{1}{2}) N(N+1) \lambda^2 \omega_0 + \frac{1}{2} (v + \frac{1}{2}) \frac{1}{V_M''} V_{\text{SME}}^{e''} \omega_0 \\
&\quad + \frac{1}{16} (v + \frac{1}{2})^2 \frac{1}{V_M''} R_0^2 (V_M^{(4)} + V_{\text{SME}}^{e(4)}) \lambda \omega_0 . \tag{B.8}
\end{aligned}$$

We identify these as contributions to the coefficients α_0 , δ_{SME}^e and x_0 , x_{SME}^e respectively in section 5.

Next, consider the perturbations at 2nd order. Organising by the total number of factors of x occurring (recalling that each power of x carries an associated $\sqrt{\lambda}$), we first find contributions in (B.4) where both factors of δV are proportional to x ; then where both $\delta V \sim x^2$, together with a mixed term with one factor of $\delta V \sim x$ and the other $\delta V \sim x^3$; and finally, terms with $\delta V \sim x$, $\delta V \sim x^5$, $\delta V \sim x^2$, $\delta V \sim x^4$ and both $\delta V \sim x^3$, the latter three contributing leading $O(\lambda)$ terms to x_0 and x_{SME}^e .

Taking these in turn, we first evaluate the contribution to $E_v^{(2)}$ from taking the perturbation $\delta V = \left(-\lambda \omega_0 N(N+1) + R_0 V_{SME}^{e'} \right) x / R_0$. The required expectation value is

$$\sum_{k \neq v} \frac{1}{(E_v^{(0)} - E_k^{(0)})} \frac{1}{R_0^2} \langle v | x | k \rangle \langle k | x | v \rangle = -\frac{1}{2} \frac{1}{(R_0^2 V_M'')} , \quad (\text{B.9})$$

with the sum over $k = v \pm 1$. Notice that this is independent of the vibrational quantum number v . The corresponding contribution to $E_v^{(2)}$ is therefore

$$E_{v; [1,1]}^{(2)} = -\frac{1}{2} \lambda^3 (N(N+1))^2 \omega_0 + \lambda N(N+1) \frac{1}{(R_0 V_M'')} V_{SME}^{e'} \omega_0 , \quad (\text{B.10})$$

which we identify with terms in D_0 and B_{SME}^e respectively.

A similar calculation shows

$$\sum_{k \neq v} \frac{1}{(E_v^{(0)} - E_k^{(0)})} \frac{1}{R_0^4} \langle v | x | k \rangle \langle k | x^3 | v \rangle = -\frac{3}{2} \lambda \frac{1}{(R_0^2 V_M'')} (v + \frac{1}{2}) , \quad (\text{B.11})$$

and identifying the relevant perturbations δV from (B.2) we find

$$\begin{aligned} E_{v; [1,3]}^{(2)} &= -\frac{1}{2} (v + \frac{1}{2}) \frac{V_M'''}{(V_M'')^2} V_{SME}^{e'} \omega_0 + \frac{1}{2} \lambda^2 (v + \frac{1}{2}) N(N+1) \frac{R_0 V_M'''}{V_M''} \omega_0 \\ &+ \lambda^2 (v + \frac{1}{2}) N(N+1) \left(\frac{1}{2} \frac{R_0}{V_M''} V_{SME}^{e'''} + 6 \frac{1}{(R_0 V_M'')} V_{SME}^{e'} \right) \omega_0 . \end{aligned} \quad (\text{B.12})$$

These are contributions to δ_{SME}^e , α_0 and α_{SME}^e respectively.

The next contribution at 2nd order comes from terms where both $\delta V \sim x^2$, so here we need to calculate

$$\sum_{k \neq v} \frac{1}{(E_v^{(0)} - E_k^{(0)})} \frac{1}{R_0^4} \langle v | x^2 | k \rangle \langle k | x^2 | v \rangle = -\frac{1}{2} \lambda \frac{1}{(R_0^2 V_M'')} (v + \frac{1}{2}) , \quad (\text{B.13})$$

giving the energy

$$E_{v;[2,2]}^{(2)} = -\frac{3}{4} \lambda^2 (v + \frac{1}{2}) N(N+1) \frac{1}{V_M''} V_{\text{SME}}^{e''} \omega_0, \quad (\text{B.14})$$

which adds to α_{SME}^e . We have discarded the $\lambda^4 (v + \frac{1}{2}) (N(N+1))^2 \omega_0$ term here as it is not of the type for which we have kept the coefficients in (5.8).

Moving on to the 2nd order contributions with a total of 6 powers of x , we find they involve factors of $(v + \frac{1}{2})^2$, so we are only concerned here with their effect on x_0 and x_{SME}^e . In turn, these are:

$$\sum_{k \neq v} \frac{1}{(E_v^{(0)} - E_k^{(0)})} \frac{1}{R_0^6} \langle v | x^3 | k \rangle \langle k | x^3 | v \rangle = -\frac{15}{4} \lambda \omega_0 [(v + \frac{1}{2})^2 + \frac{7}{60}] \frac{1}{(R_0^2 V_M'')^2}, \quad (\text{B.15})$$

from which,

$$E_{v;[3,3]}^{(2)} = -\frac{5}{48} \lambda \omega_0 [(v + \frac{1}{2})^2 + \frac{7}{60}] \frac{1}{V_M''} R_0^2 ((V_M''')^2 + 2V_M''' V_{\text{SME}}^{e'''}), \quad (\text{B.16})$$

contributing to x_0 and x_{SME}^e ;

$$\sum_{k \neq v} \frac{1}{(E_v^{(0)} - E_k^{(0)})} \frac{1}{R_0^6} \langle v | x^2 | k \rangle \langle k | x^4 | v \rangle = -\frac{3}{2} \lambda \omega_0 [(v + \frac{1}{2})^2 + \frac{1}{4}] \frac{1}{(R_0^2 V_M'')^2}, \quad (\text{B.17})$$

giving

$$E_{v;[2,4]}^{(2)} = -\frac{1}{16} \lambda \omega_0 [(v + \frac{1}{2})^2 + \frac{1}{4}] \frac{1}{(V_M'')^2} R_0^2 V_M^{(4)} V_{\text{SME}}^{e''}, \quad (\text{B.18})$$

which contributes only to x_{SME}^e ; and

$$\sum_{k \neq v} \frac{1}{(E_v^{(0)} - E_k^{(0)})} \frac{1}{R_0^6} \langle v | x | k \rangle \langle k | x^5 | v \rangle = -\frac{15}{4} \lambda \omega_0 [(v + \frac{1}{2})^2 + \frac{1}{4}] \frac{1}{(R_0^2 V_M'')^2}, \quad (\text{B.19})$$

giving

$$E_{v;[1,5]}^{(2)} = -\frac{1}{16} \lambda \omega_0 [(v + \frac{1}{2})^2 + \frac{1}{4}] \frac{1}{(V_M'')^2} R_0^2 V_M^{(5)} V_{\text{SME}}^{e'}, \quad (\text{B.20})$$

which again only contributes to x_{SME}^e . Comparing with (5.9) and (5.19), we see that we have now reproduced exactly all the terms found in the effective potential method up to 2nd order in the perturbations.

So far, in (B.7) and (B.15), (B.17), (B.19), we have just discussed the $O(v + \frac{1}{2})^2$ contributions, keeping only the terms independent of the angular momentum since we

the effective potential and perturbation theory methods, and to verify that the terms quoted in section 5 for the rovibrational energies are *complete* at the quoted order in λ , we need to analyse more closely the systematics of the expansion in λ in this expectation value approach.

First, notice that in the perturbation series in (B.4), each power of x in the perturbations δV brings a factor of $\sqrt{\lambda}$ from its expression (B.6) in raising and lowering operators. Then from the energy denominators, each further order in δV brings with it an extra factor of $1/\omega_0 = 1/(R_0^2 V_M'' \lambda)$.

We can therefore count the relevant orders by inspection. For example, consider the D_0 coefficient. This arises first at 2nd order from (2.9) with both $\delta V_N \sim x$, so the expectation value itself is $O(\lambda/\omega_0)$ and since δV_N itself is of $O(\lambda\omega_0)$, the corresponding energy is $O(\lambda^3\omega_0)$. Remembering to extract a factor ω_0 to leave the coefficient D_0 dimensionless, we deduce immediately that $D_0 \sim \lambda^3$, as given in (2.9).

The next contribution would come from including the $O(x^3)$ term in the expansion of one of the δV_N factors. But then the expectation value would be $O(\lambda^2/\omega_0)$ and the contribution to D_0 would be $O(\lambda^4)$. We see therefore that as already indicated, the coefficient D_0 quoted in (2.9) is the leading term in a perturbative series in the small parameter λ . The same is true of all the rovibrational energy coefficients.

We can now use this power counting to understand the origin of the factors involving higher derivatives of $V_M(R)$ and why they must be included. A good example is α_0 . As we have seen above, this arises already in 1st order with $\delta V_N \sim \lambda\omega_0 x^2$. The expectation value $\langle x^2 \rangle$ is $O(\lambda)$, so we find the $E_v^{(1)}$ contribution is $O(\lambda^2\omega_0)$, giving $\alpha_0 \sim \lambda^2$. However, from (2.9) we know that this is not the complete result for α_0 which has another contribution of the same $O(\lambda^2)$ but with a factor depending on V_M''' . This arises at 2nd order, with perturbations $\delta V_N \sim \lambda\omega_0 x$ and $\delta V_M \sim V_M''' x^3$. Following the power counting rules, this $E_v^{(2)}$ contribution is $O(\lambda^2\omega_0 V_M'''/V_M'')$, giving the complete $O(\lambda^2)$ result for α_0 found in (2.9).¹⁷

What this example shows us is that in general we can find another contribution to a particular rovibrational coefficient which is of the same order in λ by going to a higher order in the SHO perturbation series (B.4) and including a correspondingly

¹⁷In keeping track of these orders, we always express the energies with a single overall factor of ω_0 , with all other occurrences of ω_0 being traded for derivatives V_M'' using the relation $\omega_0 = R_0^2 V_M'' \lambda$. This isolates the correct order in λ leaving residual factors involving ratios of derivatives of V_M as in (2.9) for α_0 ; numerically, we have found that these ratios are of $O(1)$. So this method of arranging the series correctly groups contributions of the same magnitude.

higher derivative term in the expansion of δV_M *if* (and only if) at the same time we can *reduce* the power of x from the expansion of the perturbation δV_N or δV_{SME} which specifies that coefficient. This process can obviously not be iterated indefinitely and this is why the number of terms in a rovibrational coefficient at a given order in λ is limited.

These considerations allow us to identify the perturbative origin of *all* the terms in the rovibrational coefficients quoted in section 5 and to verify that they are indeed complete.¹⁸ Notice also that the effective potential method, where we analyse the anharmonic oscillator around the minimum of the potential *including* the perturbations, is in some ways more efficient in identifying terms that otherwise require high orders in the systematic perturbation method.

¹⁸To verify this on the most complicated example, consider the expression for α_{SME}^e in (5.18). Label the terms in the order given there as (1) to (7). By inspection, their origin is as follows. At 2nd order, (1) $\delta V_N \sim x$, $\delta V_{\text{SME}}^e \sim x^3$; (2) $\delta V_N \sim x^2$, $\delta V_{\text{SME}}^e \sim x^2$; (4) $\delta V_N \sim x^3$, $\delta V_{\text{SME}}^e \sim x$. Then at 3rd order, we find the terms involving the expansion of δV_M : (3) $\delta V_N \sim x$, $\delta V_{\text{SME}}^e \sim x^2$, $\delta V_M \sim x^3$; (5) $\delta V_N \sim x^2$, $\delta V_{\text{SME}}^e \sim x$, $\delta V_M \sim x^3$; (7) $\delta V_N \sim x$, $\delta V_{\text{SME}}^e \sim x$, $\delta V_M \sim x^4$. Finally, there is one possible further term at 4th order: (6) $\delta V_N \sim x$, $\delta V_{\text{SME}}^e \sim x$, $\delta V_M \sim x^3$, $\delta V_M \sim x^3$. At this point we cannot iterate further by introducing more orders in δV_M because we cannot reduce the powers of x in δV_N and δV_{SME}^e any more. Any further terms are of higher order in λ . We have therefore found the *complete* set of terms in α_{SME}^e at its leading order in λ , *i.e.* $O(\lambda^2)$. A similar exercise readily identifies the origin of all the terms in the expression (5.19) for x_{SME}^e .

References

- [1] W. Pauli, *Phys. Rev.* **58** (1940) 716.
- [2] J. S. Bell, Birmingham University thesis (1954).
- [3] G. Lüders, *Det. Kong. Danske Videnskabernes Selskab Mat. fysiske Meddelelser* **28** (1954) no. 5.
- [4] W. Pauli, in W. Pauli, ed., “*Niels Bohr and the Development of Physics*”, McGraw-Hill, New York, 1955.
- [5] M. Charlton, S. Eriksson and G. M. Shore, “*Antihydrogen and Fundamental Physics*”, Springer, 2020; preprint [arXiv:2002.09348 [hep-ph]].
- [6] M. J. Borchert *et al.* [BASE], “*A 16-parts-per-trillion measurement of the antiproton-to-proton charge–mass ratio*”, *Nature* **601** (2022), 53.
- [7] M. Ahmadi *et al.* [ALPHA], “*Characterization of the 1S -2S transition in antihydrogen*”, *Nature* **557** (2018), 71.
- [8] M. Ahmadi *et al.* [ALPHA], “*Observation of the hyperfine spectrum of antihydrogen*”, *Nature* **548** (2017), 66.
- [9] M. Ahmadi *et al.* [ALPHA], “*Investigation of the fine structure of antihydrogen*”, *Nature* **578** (2020), 375. [erratum: *Nature* **594** (2021), E5]
- [10] M. Ahmadi *et al.* [ALPHA], “*Observation of the 1S -2S transition in trapped antihydrogen*”, *Nature* **541** (2016), 506-510
- [11] H. Muller, S. Herrmann, A. Saenz, A. Peters and C. Lammerzahl, “*Tests of Lorentz invariance using hydrogen molecules*”, *Phys. Rev. D* **70** (2004), 076004.
- [12] S. Schiller, “*Precision Spectroscopy of molecular hydrogen ions: an introduction*”, *Contemporary Physics* **63** (2022), 247 and Supplementary material.
- [13] A. Carrington *et al.*, “*Spectroscopy of the hydrogen molecular ion*”, *J. Phys. B: At. Mol. Opt. Phys.* **22** (1989) 3551.
- [14] S. Schiller, D. Bakalov and V. I. Korobov, “*Simplest Molecules as Candidates for Precise Optical Clocks*”, *Phys. Rev. Lett.* **113** (2014), 023004.
- [15] M. R. Schenkel, S. Alinghanbari and S. Schiller, “*Laser spectroscopy of a rovibrational transition in the molecular hydrogen ion H_2^+* ”, *Nature Physics* **20** (2024), 383.
- [16] D. Colladay and V. A. Kostelecky, “*Lorentz violating extension of the standard model*”, *Phys. Rev. D* **58** (1998), 116002. [arXiv:hep-ph/9809521 [hep-ph]].
- [17] A. Kostelecký and M. Mewes, “*Fermions with Lorentz-violating operators of arbitrary dimension*”, *Phys. Rev. D* **88** (2013), 096006. [arXiv:1308.4973 [hep-ph]].

- [18] V. A. Kostelecky and N. Russell, “*Data Tables for Lorentz and CPT Violation*”, Rev. Mod. Phys. **83** (2011), 11. [arXiv:0801.0287v17 [hep-ph]].
- [19] V. A. Kostelecký and A. J. Vargas, “*Lorentz and CPT tests with hydrogen, antihydrogen, and related systems*”, Phys. Rev. D **92** (2015), 056002. [arXiv:1506.01706 [hep-ph]].
- [20] G. M. Shore, “*Lorentz and CPT violation and the hydrogen and antihydrogen molecular ions II – hyperfine-Zeeman spectrum*”, Phys. Rev. D **112** (2025) 056016, [arXiv:2504.19015v3 [hep-ph]].
- [21] A. Berera and L. Del Debbio, “*Quantum Mechanics*”, Cambridge University Press, 2022.
- [22] D. A. Varshalovich and A. V. Sannikov, “*H₂⁺ molecular ions in the interstellar medium*”, Pis'ma Astron. Zh. **19** (1993), 719.
- [23] V. I. Korobov, “*Rovibrational states of H₂⁺. Variational calculations*”, Molecular Physics **116** (2017), 93. Erratum: Mol. Phys. **119** (12) (2021).
- [24] V. A. Kostelecky and C. D. Lane, “*Nonrelativistic quantum Hamiltonian for Lorentz violation*”, J. Math. Phys. **40** (1999), 6245. [arXiv:hep-ph/9909542 [hep-ph]].
- [25] T. J. Yoder and G. S. Adkins, “*Higher order corrections to the hydrogen spectrum from the Standard-Model Extension*”, Phys. Rev. D **86** (2012), 116005. [arXiv:1211.3018 [hep-ph]].
- [26] S. Alighanbari, G. S. Giri, F L. Constantin, V. I. Korobov and S. Schiller, “*Precise test of quantum electrodynamics and determination of fundamental constants with HD⁺ ions*”, Nature **581** (2020), 152.
- [27] E. G. Myers, “*CPT tests with the antihydrogen molecular ion*”, Phys. Rev. A **98** (2018), 010101(R).
- [28] J.-Ph. Karr, “*Stark quenching of rovibrational states of H₂⁺ due to motion in a magnetic field*” Phys. Rev. A **98** (2018), 062501.
- [29] M. C. Zammit *et al.*, “*Laser-driven production of the antihydrogen molecular ion*”, Phys. Rev. A **100** (2019) 042709.
- [30] M. C. Zammit, C. J. Baker, S. Jonsell, S. Eriksson and M. Charlton, “*Antihydrogen chemistry*”, Phys. Rev. A **111** (2025) 050101.
- [31] C. G. Parthey, A. Matveev, J. Alnis, B. Bernhardt *et al.* “*Improved Measurement of the Hydrogen 1S - 2S Transition Frequency*”, Phys. Rev. Lett. **107** (2011), 203001.
- [32] A. Matveev, C. G. Parthey, K. Predehl *et al.* “*Precision Measurement of the Hydrogen 1S–2S Frequency via a 920-km Fiber Link*”, Phys. Rev. Lett. **110** (2013), 230801.

- [33] V. A. Kostelecky and C. D. Lane, “*Constraints on Lorentz violation from clock comparison experiments*”, Phys. Rev. D **60** (1999) 116010, [arXiv:hep-ph/9908504 [hep-ph]].
- [34] P. Wolf, F. Chapelet, S. Bize and A. Clairon, “*Cold Atom Clock Test of Lorentz Invariance in the Matter Sector*”, Phys. Rev. Lett. **96** (2006) 060801, [arXiv:hep-ph/0601024 [hep-ph]].
- [35] H. Pihan-Le Bars, C. Guerlin, R. D. Lasserri, J. P. Ebran, Q. G. Bailey, S. Bize, E. Khan and P. Wolf, “*Lorentz-symmetry test at Planck-scale suppression with nucleons in a spin-polarized ^{133}Cs cold atom clock*”, Phys. Rev. D **95** (2017) 075026, [arXiv:1612.07390 [gr-qc]].
- [36] V. I. Korobov, L. Hilico and J.-Ph. Karr, “*Hyperfine structure in the hydrogen molecular ion*”, Phys. Rev. A **74** (2006), 040502(R).
- [37] J.-Ph. Karr, V. I. Korobov and L. Hilico, “*Vibrational spectroscopy of H_2^+ : Precise evaluation of the Zeeman effect*”, Phys. Rev. A **77** (2008), 062507.
- [38] J.-Ph. Karr, V. I. Korobov and L. Hilico, “*Vibrational spectroscopy of H_2^+ : Hyperfine structure of two-photon transitions*”, Phys. Rev. A **77** (2008), 063410.